University of South Bohemia in České Budějovice

Faculty of Science

Department of Molecular Biology

Functional analysis of novel F_1-ATPase subunit in *Trypanosoma brucei*

Master Thesis

Bc. Hana Váchová

Supervisor: RNDr. Alena Panicucci Zíková, Ph.D.

Institute of Parasitology, Biology Centre, AS CR, v.v.i.

Laboratory of Functional Biology of Protists

České Budějovice 2015

Váchová, H., 2015: Functional analysis of novel F_1-ATPase subunit in *Trypanosoma brucei*. Mgr. Thesis, in English. – 47 p., Faculty of Science, University of South Bohemia, České Budějovice, Czech Republic.

Annotation: Although F_1-ATPase is extremely conserved among organisms, a putative subunit p18 was identified in *Trypanosoma brucei* F_1-ATPase complex. To explore its function in the procylic, bloodstream and dyskinetoplastic trypanosomes, three different RNAi cell lines were created. Upon p18 silencing the F_1-moiety structural integrity was impaired suggesting that p18 is indeed a *bona fide* subunit of this complex. Since F_1-ATPase is crucial for the bloodstream form survival, its potential inhibitor from the 4-oxopiperidine-3,5-dicarboxylates class (JK-11) was examined. JK-11 inhibited growth of the bloodstream trypanosomes, decreased mitochondrial membrane potential and reduced ATPase and ATP synthase activity in mitochondrial lysates. Our results suggest that JK-11 may act on F_oF_1-ATP synthase/ATPase and its inhibition may contribute to the cytotoxicity of this drug.

Prohlašuji, že svoji diplomovou práci jsem vypracovala samostatně pouze s použitím pramenů a literatury uvedených v seznamu citované literatury.

Prohlašuji, že v souladu s § 47b zákona č. 111/1998 Sb., v platném znění souhlasím se zveřejněním své diplomové práce, a to v nezkrácené podobě elektronickou cestou ve veřejně přístupné části databáze STAG provozované Jihočeskou univerzitou v Českých Budějovicích na jejích internetových stránkách, a to se zachováním mého autorského práva k odevzdanému textu této kvalifikační práce. Souhlasím dále s tím, aby toutéž elektronickou cestou byly v souladu s uvedeným ustanovením zákona č. 111/1998 Sb., zveřejněny posudky školitele a oponentů práce i záznam o průběhu a výsledku obhajoby kvalifikační práce. Rovněž souhlasím s porovnáním textu mé kvalifikační práce s databází kvalifikačních prací Theses.cz provozovanou Národním registrem vysokoškolských kvalifikačních prací a systémem na odhalování plagiátů.

České Budějovice, 24. dubna 2015 ...……..

Hana Váchová

Acknowledgements

I take this opportunity to express my gratitude to all members of Laboratory of Functional Biology of Protist. Mainly I am grateful to Alena for supervising and introducing me into the functional and molecular biology of protists. I have to express my appreciation to Brian, Ondra, Dave, Eva, Kája, Zuzka, Honzík, Míša and Míša for excellent and funny working environment. I also thank my parents and friends for the encouragement, support and attention. I am also grateful to my quinea-pig Sophie for moral and fluffy support.

Obsah

1. Introduction

1.1. *Trypanosoma brucei*

1.1.1. The organism *Trypanosoma brucei*

Trypanosoma brucei belongs to the family Kinetoplastidae, clade Euglenozoa (Simpson and Roger, 2004). It is flagellated protozoan parasite with a body formed by a single cell. Importantly, *Trypanosoma brucei* is itself divided into three subspecies namely *T. brucei brucei, T. b. gambiense* and *T. b. rhodesianse*. These parasites are transmitted by blood-sucking tsetse flies (*Glosina* genus) and cause worldwide devastating and neglected diseases in humans and animals (Stuart *et al*., 2008).

Trypanosoma brucei brucei is found in entire Sub-saharan Africa. This parasite is not able to infect humans due to its inability to survive the lysis by a lytic factor present in normal human serum, called trypanosome lytic factors (TLF) (Thompson *et al*., 2009). Thus *T. brucei brucei* is a primary parasite of native antelopes and other wild ruminants but also infects domestic animals. This disease is called nagana or animal African trypanosomiasis (AAT) and has an economic impact on the agriculture development in Africa (Kennedy, 2013).

Trypanosoma brucei rhodesiense, found in Eastern and Southern Africa, is infective to humans. It has evolved the serum resistence protein called SRA making it resistant to lysis by TLF´s (De Greef and Hamers, 1994). Importantly, *T. b. rhodesiense* causes an acute, rapidly progressive infection called Rhodesiense human African trypanosomiasis. Infection requires a non-human reservoir (wild or domestic animals) for maintaining its population (Stuart *et al*., 2008).

Trypanosoma brucei gambiense, found in West and Central Africa, does not have SRA genes but has evolved other mechanism to protect itself before lysis by TLF´s (Kieft *et al*., 2001). Disease is called Gambiense human African trypanosomiasis and progresses at slower rate. The main reservoirs are other human beings (Stuart *et al*., 2008), but rarely infecte both domestic and wild animals (Nijokou *et al*., 2006; Nijokou *et al*., 2010).

1.1.2. Life cycle

T. brucei life cycle is relatively complex (Figure 1.1). In that, parasites undergo dramatic changes in two-phase life cycle such as various different stages, distinctive morphology, and biochemical physiology between mammalian hosts and insect vectors (Besteiro *et al*., 2005).

During the life cycle of *T. brucei*, tsetse fly bites infected animals or humans and ingests a bloodmeal containing trypanosomes. The procyclic forms (PF) replicate in the insect´s midgut and migrate to the salivary gland, where they undergo a complex series of biochemical and morphological changes into the infectious metacyclic forms. Metacyclic forms are then injected by a tsetse bite during blood meal in host and initially proliferate at the site of injection. Parasites differentiate into long, slender bloodstream forms (BF) and replicate in the host bloodstream. These forms are able to change antigenic variation by variant surface protein (VSG) allowing them to escape antibody-mediated killing and evade the host (Horn and McCulloch, 2010).

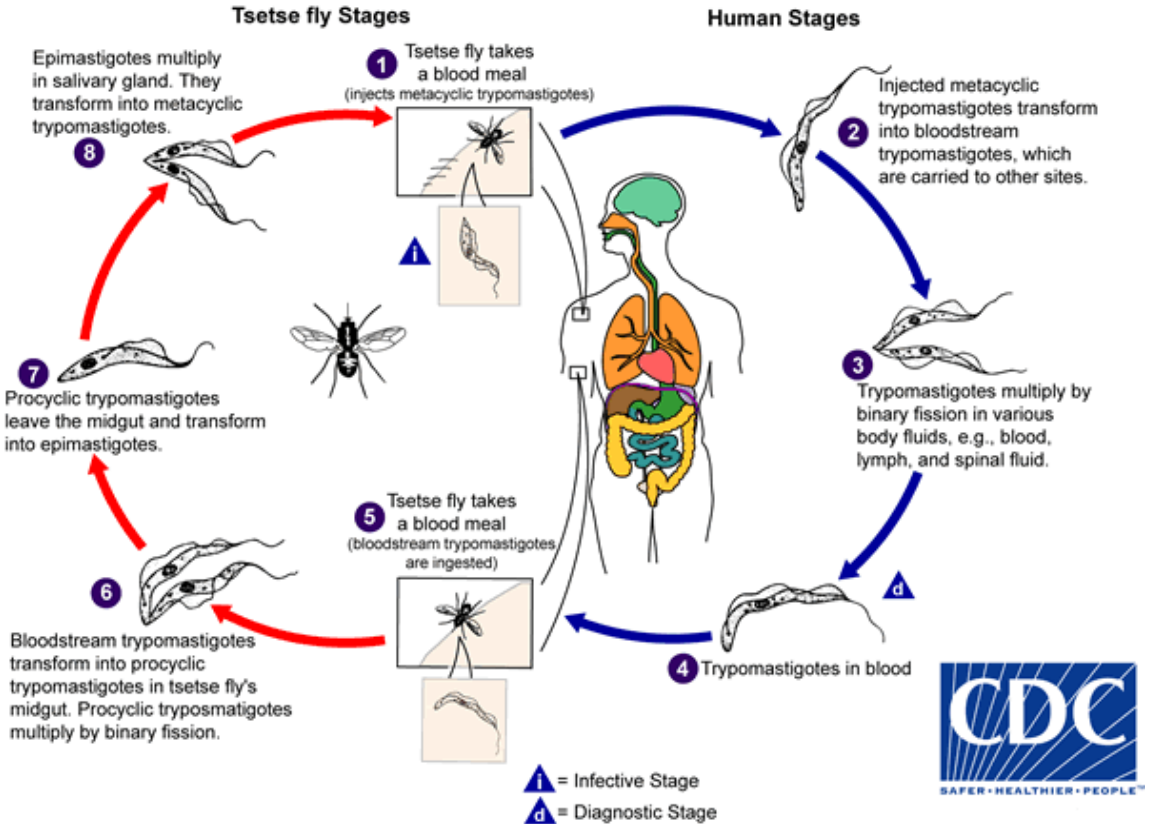

Fig. 1.1: *T. brucei* undergoes a complex life cycle (http://www.cdc.gov/dpdx/trypanosomiasisAfrican/index.html).

1.1.3. Human African trypanosomiasis

Human African trypanosomiasis (HAT), so called sleeping sickness, is one of the most neglected diseases worldwide. In 1995, 300000 new cases were reported per year, but only 30000 of them were treated (Simarro *et al*., 2011). Due to a vector control and available treatment, number of reported infected cases was reduced in 2009 when less then 10000 cases were reported (Simarro *et al*., 2011). Not only in Africa but also in the USA and Europe, the HAT cases are documented mainly due to travelling. Between 2000 and 2010 there were 94 cases of HAT reported in these countries (Kennedy, 2013).

The clinical features of HAT depend on the parasite species, the stage of the disease and the host. The signs and symptoms are generally the same for both forms of the disease but differ in their frequency, seriousness and progress. The more common West African disease (97% of cases), caused by *T. b. gambiense*, is characterized by a chronic progressive course (Kennedy, 2013) that is usually fatal if untreated or inadequately treated (Jamoneau *et al*., 2012). Contrarily, the less common east African disease (3% of cases) caused by *T. b. rhodesiense* is usually an acute disease, which progresses to second stage within a few weeks and to death within 6 months (Kennedy, 2013).

The disease occurs in two stages, the first (haemolymphatic) stage and the second (meningoencephalitic) stage with invasion of the CNS by the trypanosomes. Early stage symptoms are usually unspecific and include headache, arthralagia, weight loss, and fatigue. Later are observed various features such as enlargement of the spleen or liver, myocarditis, pericarditis, iritis, keratitis, and endocrine dysfunctions. The other symptoms include neurological signs and sleep disturbances giving the disease its name (Kennedy, 2013).

1.1.4. Medical treatment of sleeping sickness

Although, there is a significant progress in the knowledge of biology of this parasite and pathophysiology of sleeping sickness, no new drugs were developed to treat this disease during the last 25 years. More than disturbing is fact that available drugs are obsolete, toxic, have various efficiency, and long treatments. Mainly financial limit represents significant obstacle in developing of new drugs against sleeping sickness.

Nevertheless, there are some drugs commonly used against sleeping sickness. Their use depends on type of sickness, line treatment and the stage of the disease. Different drugs are used against Gambiense HAT and the others are used against Rhodesiense HAT (Kennedy, 2013). Drugs are divided into 2 groups – first and second line of treatments (Table 1.1). The first line of treatment is applied immediately after expressing of symptoms. This kind of treatment is dispensed regularly for long time. The second line of treatment is used when insufficient response or side effects drugs of the first line treatment are occurred.

Tab. 1.1: Drugs used for treatment of sleeping sickness (Kennedy, 2013).

Disease	First line treatment	Second line treatment
Early stage		
Rhodesiense HAT - *T. b. rhodesiense*	Suramin	Pentamidine
Gambiense HAT - *T. b. gambiense*	Pentamidine	Suramine
Late stage		
Rhodesiense HAT - *T. b. rhodesiense*	Melarsoprol	None available
Gambiense HAT - *T. b. gambiense*	Eflorniothine and Nifurtimox	Melarsoprol

For treatment of the first stage of Rhodesiense HAT is commonly used suramin. This drug was discovered in 1921. The mechanism of action is unknown and provokes certain undesirable effects such as renal failure, skin lesions, anaphylactic shock, bone marrow toxicity and peripheral neuropathy (Kennedy, 2013). For treatment of the early stage of Gambiense HAT, pentamidine was first used in 1940. Mechanism of its action is not fully understood with significant undesirable effects. Pentamidine can be easily overdosed with symptoms including pain, nausea, fever, rash, hallucinations, dizziness and diarrhea (Kennedy, 2013).

For treatment of the late stage of both Rhodesiense and Gambiense HAT is commonly used melarsoprol discovered in 1949. This drug has known mechanism of action that acts against trypanothione, a unique parasitic enzyme responsible for regulation of the thiol/disulfide redox balance (Fairlamb *et al*., 1989). Unfortunately, melarsoprol is extremely toxic because of its derivation from arsenic compounds and thus has many undesirable side effects. The most dramatic is encephalopathic syndrome which can be fatal (Kennedy, 2013). On the other side, eflornithine, a potential inhibitor of ornithine decarboxylase in polyamine pathway (Bacchi *et al*., 1980), is used only against Gambiense HAT. It is less toxic than melarsoprol but still might have several side effects such as bone marrow toxicity and gastrointestinal symptoms. This drug was mainly used from 1990 until 2009. Since 2009 eflornithine is used frequently in combination with nifurtimox (Kennedy, 2013).

Although, financial limits represent significant obstacle in developing new drugs against sleeping sickness and thus it is not so attractive for pharmaceutical company to support these efforts, there are some new potential drugs in pipeline at various stages of development. The most recent promising candidate, DB289 is orally administered drug for early stage of HAT. However ADMET studies revealed its toxicity for liver and kidney cells and thus this drug was abondoned (Pholig *et al*., 2008). Neverthelss, there are more

promising candidates, such as fenixidazole or SCYX-7158. Both of these drugs were successfully tested in pre-clinical trials. So far, neither fenixidazole nor SCYX-7158, do not evince any side effects and toxicity (Kennedy, 2013).

1.2. Mitochondria

Mitochondria are unique organelles described as the powerhouse of the cell because they generate adenosine triphosphate (ATP) used as a source of chemical energy for the most of the cell activities. Because of mitochondria consume oxygen and release carbon dioxide, whole process is known as cellular respiration and takes place in mitochondrial respiratory chain (Alberts *et al*., 2008).

Mitochondrial respiratory chain is composed from 5 different protein complexes responsible for electron transport, generation of proton gradient and ATP synthesis. The complexes responsible for these actions are located in the inner mitochondrial membrane and are known as mitochondrial complexes I – V. Complexes I – IV contain subunits with attached metal ions (for instance Fe-S clusters) or hemoproteins, which are responsible for passing electrons down the redox potential to a final electron acceptor, oxygen. Complex I (NADH coenzyme Q reductase) accepts electrons from NADH (nicotine adenine dinucleotide) and passes them to coenzyme Q (ubiquinone) which also receives electrons from complex II (succinate dehydrogenase) that accepts electrons from succinate. Coenzyme Q passes electrons through complex III (cytochrom bc_1) to cytochochrom c and finally to complex IV (cytochrom c oxidase). Complex IV uses the electrons and hydrogen ions to reduce oxygen to water. The whole process of electron movements is coupled with translocation of H^+ across the inner membrane and thus generating the electrochemical proton gradient. This proton gradient allows complex V (F_oF_1-ATP synthase) to use the flow of H^+ through the enzyme back into the matrix to synthesize ATP from adenosine diphsophate (ADP) and inorganic phosphate (Pi) (Alberts *et al*., 2008).

1.2.1. *T. brucei* mitochondrion

Mitochondrion of *T. brucei* is unique in many aspects. Interestingly, mitochondrion is present in one copy per cell. Its DNA is located at the posterior end of the mitochondrion and is known as kDNA or kinetoplast. Kinetoplast is a network of DNA composed from 2 forms of circular DNA, maxicircles and minicircles. Maxicircles are between 20 and 40 kb in size present in a few dozen per kinetoplast. They encode typical protein products needed for the mt ribosomes and oxidative phosphorylation pathway. On the other hand, minicircles are between 0.5 and 1 kb in size present in a several thousands minicircles per kinetoplast.

Their only known function is to produce guide RNA (gRNA) to decode the encrypted maxicircle information. It happens through the insertion or deletion of uridine residues (Simpson *et al*., 2000; Simpson *et al*., 2003) and by process known as RNA editing.

The mitochondrial function, size and activity differ between the life stages of *T. brucei*. Thus, three different forms of the mitochondrion are recognized. The PF stage contains active mitochondrion with cristae and fully developed mitochondrial respiratory chain (Besteiro *et al*., 2005), while the BF stage possesses a mitochondrion strongly reduced in size and activity (Schnaufer *et al*., 2002). Third form includes mitochondrion present in the BF stage that lost its kDNA (Stuart, 1971). These trypanosomes are called dyskinetoplastic (partial loss of kDNA) or akinetoplastic (a complete loss of kDNA) and can be found in nature (*T. equiperdum* and *T. evansi*) (Brun *et al*., 1998) or in the labs (Dk164) (Stuart, 1971)

1.2.1.1. Mitochondrion of the bloodstream form

The BF of *T. brucei* live in the blood of its mammalian host. Since the blood is rich in glucose, BF mitochondrion has only a minor role in energy metabolism and thus is dramatically reduced (Figure 1.2 b). After the transmission to the mammalian host, parasite stops producing ATP by oxidative phosphorylation and switches to simpler and less effective production of ATP by glycolysis (Coustou *et al*., 2003; Hannaert *et al*., 2003). Therefore, mitochondrion lacks cristae and Krebs cycle enzymes are missing as most of the respiratory chain complexes that maintain the mitochondrial membrane potential (Hannaert *et al*., 2003; Schnaufer *et al*., 2005).

Although, key enzymes of Krebs cycle and respiratory complexes III and IV are missing, mitochondrion still possesses its essential function (Schnaufer *et al*., 2002). Examples of some of the essential processes are calcium ion homeostasis, iron-sulphur cluster synthesis and production of acetate for fatty acid biosynthesis (Nolan and Voorheis, 1992; Mazet *et al*., 2013; Kovářová *et al*, 2014). The reduced mitochondrial NADH molecules are probably reoxidized by the activity of complex I or by alternative dehydrogenase (Fang and Beattie, 2003; Verner *et al*., 2011). The final acceptor of electron is a trypanosome specific alternative oxidase (TAO) (Chaudhuri *et al*., 1998), which also accepts electrons from glycerol-3-phosphate dehydrogenase via ubiquinone. This enzyme is important for maintaining the glycosomal redox balance through glycerol-3-phosphate/dihydroxyacetone shuttle (Opperdoes *et al*., 1977). However none of these activities generates mitochondrial membrane potential that is known to be essential for every

eukaryotic cell containing aerobic mitochondrion. Thus, uniquely in trypanosome, the mitochondrial membrane potential is generated by a hydrolytic activity of the complex V, F_oF_1-ATPase (Nolan and Voorheis, 1992; Schnaufer *et al*., 2005).

1.2.1.2. Mitochondrion of the procyclic form

In contrast to BF mitochondrion, the PF organelle is fully developed resembling a typical aerobic mitochondria (Acestor *et al*., 2009). It contains enzymes of the Krebs cycle, (Figure 1.2 c) and a fully functional respiratory chain (Figure 1.2 a) (Besteiro *et al*., 2005).

Interestingly, the Krebs cycle does not operate as a cycle, but the reactions are used just partially (van Weelden *et al*., 2006) (Figure 1.3). By these reactions, the main substrates, prolin and threonine, are converted to acetate and succinate. Interestingly, these reactions are coupled with ATP production by substrate phosphorylation, which plays an essential role in ATP generation in PF *T. brucei* cells (Coustou *et al*., 2003).

The respiratory chain includes typical respiratory complexes I, II, III and IV and it is involved in mt membrane potential generation. The proton gradient is then coupled to ATP synthesis by complex V (Besteiro *et al*., 2005). In addition to conventional respiratory chain, the trypanosomes mitochondrion also possesses an alternative pathway composed of alternative dehydrogenase and alternative oxidase (Chaudhuri *et al*., 1998; Fang and Beattie, 2003).

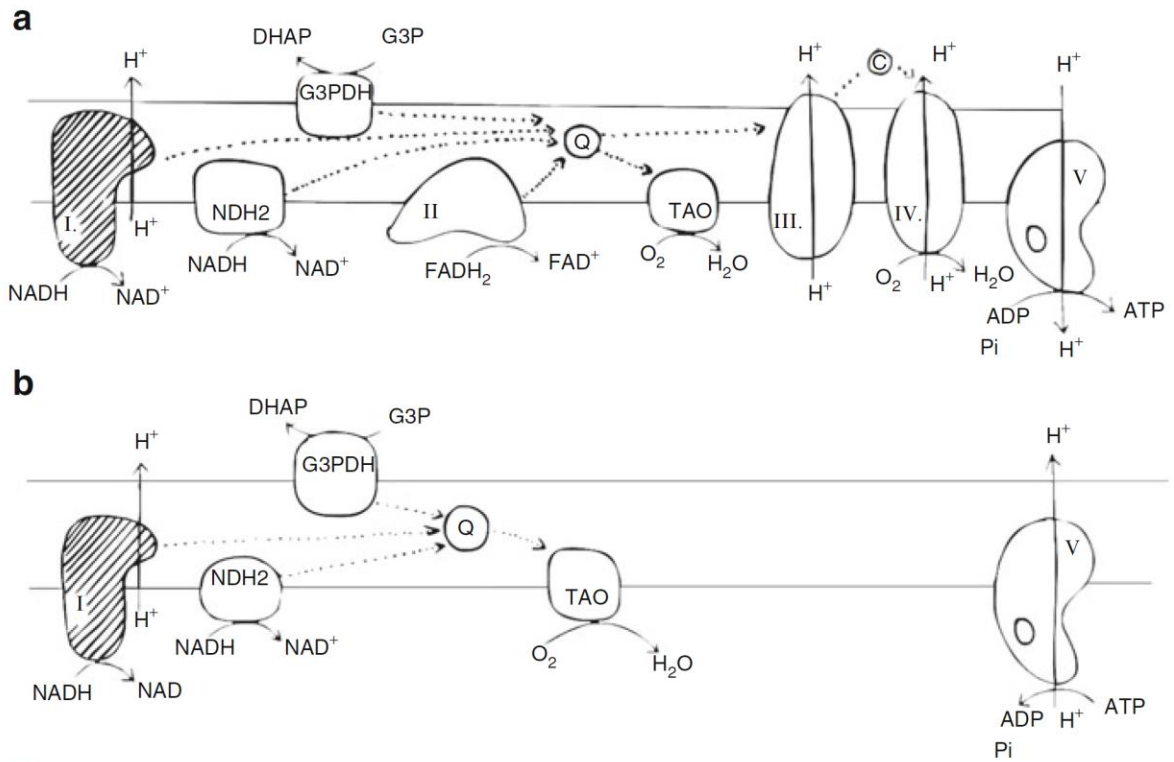

Fig. 1.2: Respiratory chains in mitochondrion of PF and BF *T. brucei* (Lukeš *et al*., 2010). A is respiratory chain of PF *T.brucei*. B is Respiratory chain of BF *T. brucei*.

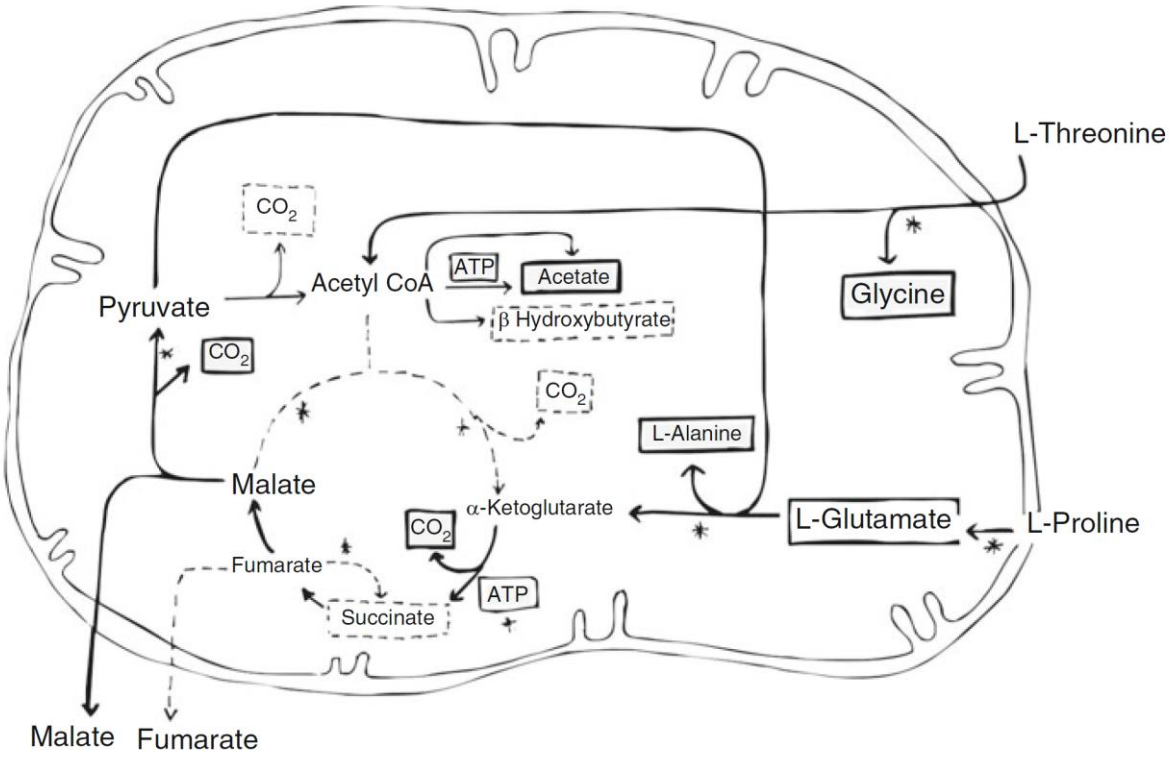

Fig. 1.3: Krebs cycle in mitochondrion of PF *T. brucei* (Lukeš *et al*., 2010).

1.3.F_oF_1-ATP synthase

F_oF_1-ATP synthase is evolutionary very old and conserved complex found in the bacterial plasma membranes, inner mitochondrial membrane, and chloroplasts of plants and algae. Its major function is to synthesize ATP from ADP and Pi (Boyer, 1997).

1.3.1. The structure of F_oF_1-ATP synthase

Prokaryotic ATP synthase (Figure 1.4b) is located on bacterial plasma membrane. It is composed from 2 parts, F_o and F_1 moieties which are linked together by a central stalk and a peripheral stalk. The prokaryotic complex from *E. coli* contains 8 different subunits stochiometrically marked as $\alpha_3\beta_3\gamma\varepsilon\delta ab_2c_{9\text{-}12}$. Interestingly, the genes for all 8 subunits are organized in a single operon called the unc operon (Walker *et al*., 1984). The catalytic F_1-moiety is composed of alternating subunit α and β creating a mushroom-like structure. This catalytic headpiece is connected to the membrane via a peripheral stalk consisting of 2 subunits, b and δ. One end of the peripheral stalk is anchored to the membrane while the second end is bound to the N-terminal part of F_1 part. The main function of this stalk is to prevent rotation of the F_1-headpiece upon a rotation of the central stalk. The central stalk is composed from the subunits γ and ε, and connects F_1 and F_o parts. F_o-part creates so called proton channel and is composed of 10 copies of subunits c. These subunits form a ring that interacts with subunit a, creating a pore for H^+ translocation (Capaldi *et al*., 2000).

Eukaryotic F_oF_1-ATP synthase (Figure 1.4a) is situated on the mitochondrial inner membrane. Although F_1-ATPase is extremely conserved, mitochondrial F_o-moiety has gained several new subunits in comparison with bacterial ATP synthase during the eukaryotic evolution (Devenish *et al*., 2008). One of the mammalian ATP synthase is bovine ATP synthase from *B. Taurus* composed of 16 subunits. The F_1-ATPase consists of 5 subunits – $\alpha_3\beta_3\gamma\delta\varepsilon$. The F_o-part is composed of subunits a, b, c, d, e, f, g, OSCP, F_6 and A6L (Collinson *et al*., 1994). The central stalk is then formed by subunits γ, δ and ε (Abrahams *et al*., 1994). The peripheral stalk is composed from subunits b, d, OSCP and F6 (Walker and Dickson, 2006). As was described for prokaryotic ATP synthase, one end of the peripheral stalk is anchored to the membrane while the second end binds to the N-terminal part of subunit α of F_1-part. The central stalk connects F_1 and F_o parts. The function of the central stalk is to transfer the energy of passing protons to ATP synthesis. Subunits a and c are linked to the proton translocation (Collinson *et al*., 1994; Walker and Collinson, 1994).

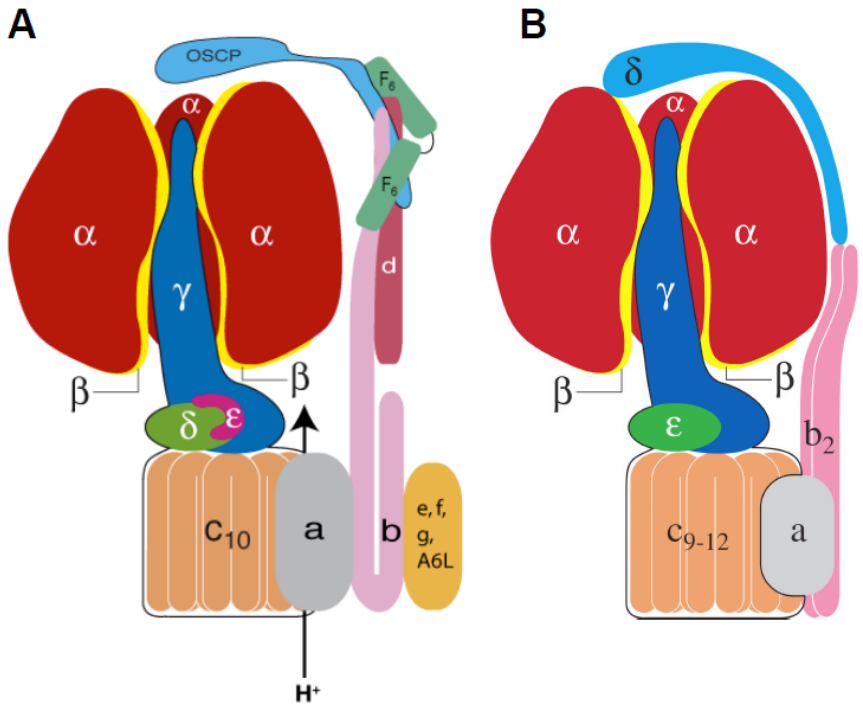

Fig.1.4: Model of mitochondrial and eubacterial ATP synthase (Bason, 2008). A represents the mitochondrial ATP synthase. B represents the eubacterial ATP synthase. In both models, subunit β has been removed to expose the central stalk of the complex.

1.3.2. The function of F_oF_1-ATP synthase

The synthesis of ATP by rotation of the enzymatic complex V was suggested by Peter Dennis Mitchell in 1961 in his chemiosmotic theory. This theory explains how the oxidation of reduced cofactors is coupled with synthesis of ATP (Mitchell, 2011).

The gained energy from oxidation of cofactors in the respiratory chain is first used for active transport of hydrogen ions through the inner mitochondrial membrane to the inner membrane space. In mitochondrial matrix there is less H^+ and thus it possesses more negative charge against cytosol. It leads to the establishment of the proton motive force that forces H^+ return back to the matrix. This reverse transport of H^+ is allowed by the ATP synthase that uses the released energy to synthesize ATP (Mitchell, 2011).

The synthesis of ATP is accomplished by a rotation of the c ring and the central stalk, that is triggered by proton translocation at the boundary of c ring and subunit a. Rotation of the central stalk is balanced by the peripheral stalk that has function as a stator (Rubinstein *et al*., 2003; Dickson *et al*., 2006). The asymmetric subunit γ rotates by 120° steps and causes 3 individual conformations changes in the catalytic sites of subunit β. Every subunit β has different affinity to nucleotides (Figure 1.5). For instance, β_{DP} (tight conformation) binds ADP, second subunit β_{TP} binds ATP (free conformation) and third subunit β_E (empty conformation) doesn´t bind any nucleotide and remains empty (Abrahams *et al*., 1994).

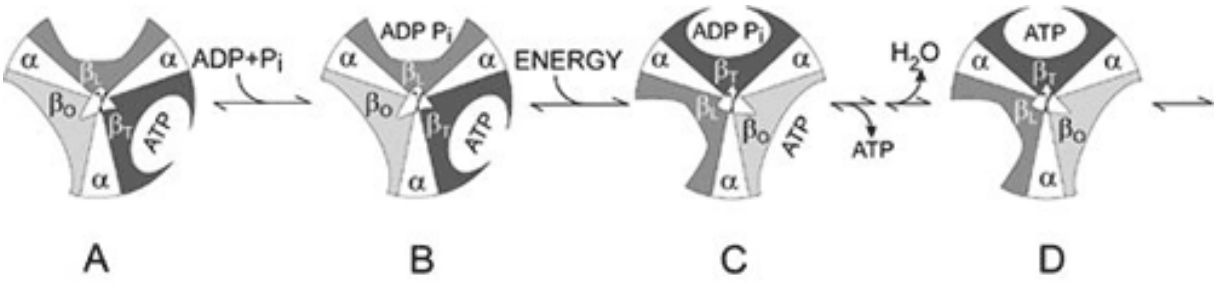

Fig. 1.5: Mechanism of ATP synthesis by Paul D. Boyer
(http://www.nobelprize.org/nobel_prizes/chemistry/laureates/1997/press.html).

ATP synthase represents reversibly coupled device. It can either use proton flows by the gradient of the electrochemical potential for ATP synthesis or pumps protons against their electrochemical gradient and generates mitochondrial membrane potential at the expenses of ATP. Synthesis or hydrolysis of ATP depends on the size of the electrochemical gradient across the membrane. For instance, if the cell is somehow exposed to low oxygen concentration, then the mitochondrial electrochemical gradient fails and the F_oF_1-ATP synthase switches from synthesis of ATP to ATP hydrolysis of ATP to maintain the mitochondrial membrane potential (Classen *et al*., 1989). Some bacterial ATP synthases consume ATP generated by glycolysis to pump proton across the plasma membrane to provide a proton gradient. This proton gradient is then used to import essential nutrients by active transport (Michels *et al*., 1979).

1.3.3. *T. brucei* F_oF_1-ATPase/ATP synthase

T. brucei F_oF_1-ATP synthase contains up to 22 subunits. Only the core F_1 subunits (α, β, γ, δ, ε), OSCP and subunits c and a were detected at the gene or protein level. In addition to these known subunits, 14 extra subunits have been identified as components of F_oF_1-complex (Zíková *et al*., 2009). Interestingly, most of them are unique to Euglenozoa clade (Perez *et al*., 2014) and have no homologues outside this group of eukaryotes. Considering the unique composition of the *T. brucei* F_oF_1-complex and its reversed function, this complex represents a potentially promising drug target.

1.4. 4-oxopiperidine-3,5-dicarboxylates

The 4-oxopiperidine-3,5-dicarboxylates are chemical compounds that strongly inhibit the *in vitro* and *in vivo* growth of medically important parasites such as *Trypanosoma brucei*, *Plasmodium falciparum* and *Leishmania major (*Goebel *et al*., 2008*)*. These compounds target enzymes of polyamine pathway, mainly hypusine biosynthesis pathway (Goebel *et al*., 2008). Hypusine, the unusual amino acid, is a product of a unique posttranslational modification of eukaryotic translation initiation factor 5A (eIF5A). This amino acid is synthesized by 2 sequential steps. In the first step, deoxyhypusine synthase (DHS) transfers 4-aminobutyl moiety of the polyamine spermidine to a specific lysine residue in the eIF5A precursor protein and forms deoxyhypusine (Park and Wolf, 1988). In the second step, deoxyhypusine is hydroxylated by deoxyhypusine hydroxylase (DOHH) to hypusine (Abbruzzese *et al*., 1986). Just DOHH is inhibited by 4-oxopiperidine-3,5-dicarboxylates. Although these compounds affect growth of these parasites, they show low cytotoxicity against macrophages. Thus, none of those drugs inhibit mammalian enzymes (Goebel *et al*., 2008).

JK-11 represents a class of these chemical compounds (Figure 1.6). Interestingly, it has been shown that treatment by this compound affects also $\Delta\psi m$ and thus interferes with the proper mitochondrial function. In order to get better insight into the cytotoxicity of these compounds, we decided to test if JK-11 inhibits function of F_oF_1-ATPase.

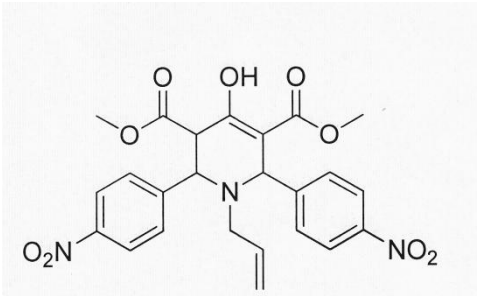

Fig. 1.6: The chemical structure of JK-11 compound.

2. Aims

- Investigate function of a novel F_1-ATPase subunit p18.
    - Generate RNAi cell line to specifically knock-down p18 expression in PF, BF and DK *T.brucei* cells.
    - Verify efficiency of PF RNAi$^{p18/p2T7\text{-}177}$, BF RNAi$^{p18/p2T7\text{-}177}$, Dk RNAi$^{p18/\ p2T7\text{-}177}$ and Dk RNAi$^{p18/pAZ0055}$ cell lines.
    - Measure $\Delta\psi m$ in PF RNAi$^{p18/p2T7\text{-}177}$, BF RNAi$^{p18/p2T7\text{-}177}$, Dk RNAi$^{p18/\ p2T7\text{-}177}$ and Dk RNAi$^{p18/pAZ0055}$ cell lines.
    - Determine structural integrity of F_oF_1-ATPase/ATP synthase complex in PF RNAi$^{p18/p2T7\text{-}177}$ and BF RNAi$^{p18/p2T7\text{-}177}$cell lines.
- Investigate mode of action of JK-11.
    - Determine EC_{50} values for JK-11 compound for PF427, BF427 and Dk164 cells *T.brucei*.
    - Measure $\Delta\psi m$ in these cells upon a treatment with different concentration of JK-11.
    - Measure the rate of ATP hydrolysis in PF cells *T. brucei* upon a treatment with JK-11.
    - Measure the level of ATP production of PF cells *T. brucei* upon a JK-11 treatment.

3. Material and methods

3.1. Functional characterization of a novel F_1-ATPase subunit p18

3.1.1. Cloning methodology

3.1.1.1. Primer design and polymerase chain reaction (PCR)

A 452bp region of the *T. brucei* p18 gene including 3' untranslated regions (3'UTR) (Tb927.5.1710) (Figure 3.1) was amplified by PCR from genomic DNA using primers showed in Table 3.1, restriction sites are underlined.

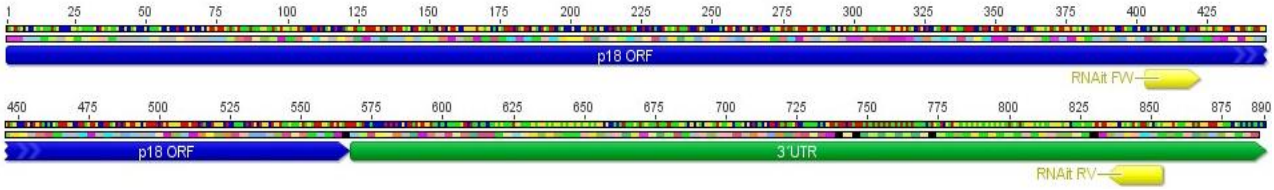

Fig. 3.1: Region of *T.brucei* p18 gene. Blue line represents an open reading frame of p18 gene. Green line represents the 3' untranslate region. Yellow lines represent sites for forward or reverse primer binding.

Tab. 3.1: List of used oligonucleotides.

Vector	Type	Restriction sites	Sequences
p2T7-177 (head to head)	FW	BamHI	GCAGGATCCCTCGGCTACTGCATTCAACA
	REV	HindIII	GACAAGCTTACAGCATTACTACACGCCCC
pAZ0055 (stem loop)	FW	SmaI and XhoI	TTTCTCGAGCCCGGGCTCGGCTACTGCATTCAACA
	REV	BamHI and XBaI	TTTTCTAGAGGATCCACAGCATTACTACACG

The PCR was carried at Thermal Cycler (Biorad) under following conditions:

1. Denaturation 94°C 2 minutes
2. Denaturation 94°C 15 seconds
3. Primer annealing 55°C 15 seconds
4. Amplification 70°C 30 seconds

} 34x

5. Amplification 70°C 2 minutes
6. Hold at 4°C

PCR products were visualized on the 0.8% agarose gel, the proper size was checked using a known DNA ladder (Invitrogen), and the amplified DNA was extracted from the gel using Sigma Gel Extraction kit (Sigma).

3.1.1.2. pGEM T-easy cloning and *E.coli* transformation

The purified PCR products were ligated into pGEM T-easy vector system (Promega) according to manufacturer's protocol.

Competent cells Xl1-blue were gently thawed on ice for 20 minutes. Ligation reaction (3 µl) was carefully mixed with 50 µl of the competent cells. Cells were incubated on ice for 10 minutes followed by a heat shock at 42°C for 45 seconds. After the heat shock, the cells were immediately cooled on ice for 2 minutes, mixed with SOC medium (250 µl) and incubated in the shaking incubator in 37°C for 45 minutes. In the meantime, 50 µl of 100 mM IPTG and 40 µl of X-gal (20 mg/ml) were added to the agarose plate containing ampicillin (100 µg/ml). The transformed cells were then spread on LB agar plate and left in an incubator overnight at 37°C. Subsequently, plasmid DNA was isolated from 6 white colonies using GenElute™ Plasmid Miniprep Kit (Sigma). The DNA was then digested with appropriate restriction enzymes, the resulting DNA fragments were analyzed on a 0.8% agarose gel and plasmids were finally verified by sequencing.

3.1.1.3. Ligation of p18 region to RNAi vectors p2T7-177 and pAZ0055

For RNAi purposes in *T. brucei*, two different vectors were used. First vector (p2T7-177), containing head to head T7 promoters, is often employed to trigger ds RNA synthesis in the *T. brucei* cell (LaCount *et al*., 2000). Second vector (pRPhyg-iSL) containing only one promoter is responsible to drive expression of the stem loop dsRNA (Alsford and Horn, 2008). This plasmid is assumed to be slightly more efficient at knocking-down mRNA levels and might be less sensitive to a leake expression without the trigger in the media. The reason for the reduced leaky expression may be that this stem-loop vector uses a procyclin promoter rather than the more powerful T7 promoter (Duran-Dubief *et al*., 2003). The vector pRPphleo-iSL (Alsford and Horn, 2008) was modified in our laboratory as the original selectable marker was removed and replaced with phleomycin. In our plasmid database, the plasmid is now called pAZ0055.

Vectors p2T7-177 (Figure 3.2) and pAZ0055 (Figure 3.3) were cleaved with particular restriction enzymes (Table 3.2). Restrictions were verified on the 0.8% agarose gel, and digested vectors were purified from the gel. Ligation of the p18 RNAi regions followed using a regular ligation conditions. The ligation reaction was then treated in the same way as described for pGEM-T easy cloning.

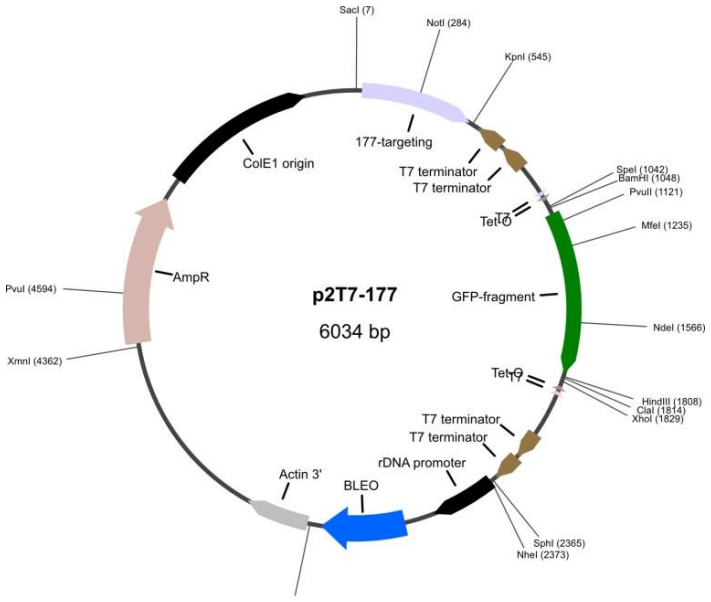

Fig. 3.2: Map of p2T7-177 vector.

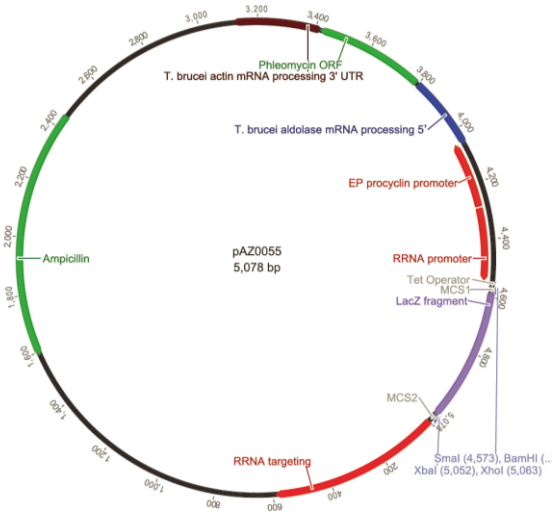

Fig. 3.3: Map of pAZ0055 vector.

Tab. 3.2: List of used vectors for cloning RNAi constucts.

Type	Vector	Fragment	Restriction sites
Head to head	p2T7-177	1st	HindIII, BamHI
Stem loop	pAZ0055	1st	SmaI, BamHI
		2nd	XbaI, XhoI

The final plasmids containing the p18 RNAi region were verified by sequencing. In order to transfect *T. brucei*, the final plasmids (p18/p2T7-177 and p18/pAZ0055) were linearized using NotI restriction enzyme.

3.1.1.4. Transfection to *T. brucei* PF 29-13

PF cells 29-13 in mid-log phase (total cell number $1x10^8$ cells) were harvested (1300 g, 4°C, 10 minutes). The cell pellet was washed twice with 10 ml of ice cold CytoMix buffer and then resuspended in 1 ml of the same buffer. Linearized, sterile DNA (10 µg) was loaded into a 0.2 cm gap cuvette (Electroporation Cuvettes Plus Model no. 620, BTX) and the cell suspension (500 µl) was added. The mixture was treated with one pulse (1600 V, 25 Ω, 50 µF) using the ECM630 PrecisionPulseTMelectroporator (BTX-Genetronics). Cells were then resuspended in 6 ml SDM-79 medium with 10% FBS (fetal bovine serum) containing hygromycine (H) and G418 antibiotics, and incubated overnight at 27°C. After 16 hours, the selectable antibiotic (phleomycin) was added at a concentration of 2.5 µg/ml. The cells were then serially diluted into a 24-well plate to facilitate the cloning of transfectants with the integrated RNAi vector.

3.1.1.5. Transfection to *T.brucei* BF SM and *T.evansi*

BF SM and *T. evansi* cells in mid-log phase (total cell number $3x10^7$ cells) were harvested (1300 g, RT, 10 minutes). The cell pellet was washed once with 20 ml of sterile PBS-G and then resuspended in AMAXA Human T-cell solution (100 µl). Cells were placed into the electroporation cuvette. Precipitated linearized plasmid DNA (10 µg) was added. Electroporation was conducted using the Nucleofector II (Amaxa) X-001 program, after which the transfected cells were transferred to 30 ml HMI-9 with 10% FBS containing G418 antibiotic for BF SM cells or 30 ml HMI-9 with 10% FBS containing hygromycine and G418 antibiotics for *T.evansi* cells. Transfected cells were dispensed in 10-fold serial dilutions into 24-well plates and incubated overnight at 37°C in 5% CO_2. After 16 hours, the selectable antibiotic (phleomycin) was added at a concentration of 2.5 µg/ml.

3.1.2. Growth curves of RNAi^{p18} cell lines

T. brucei PF RNAi$^{p18/p2T7\text{-}177}$ cell lines were grown in 10 ml of SDM-79 GHPhleo medium + 10% FBS. *T. brucei* BF RNAi$^{p18/p2T7\text{-}177}$ cell lines were grown in 5 ml of HMI-9 GPhleo medium + 10% FBS. *T. evansi* RNAi$^{p18/p2T7\text{-}177}$ and RNAi$^{p18/pAZ0055}$cell lines were grown in 5 ml of HMI-9 GHPhleo medium + 10% FBS.

To start a growth analysis, cells were first divided into two different flasks marked as noninduced and induced. Induced cells were then induced by tetracycline at final concentration 1 µg/ml. Each day, cells were counted by the Z2 Particle Counter (Beckam Coulter Inc.) and splitted down to $3x10^6$ cells/ml for PF RNAi$^{p18/p2T7\text{-}177}$ cells, to $1x10^5$ cells/ml for BF RNAi$^{p18/p2T7\text{-}177}$ cells, to $2x10^5$cell/ml for Dk RNAi$^{p18/p2T7\text{-}177}$ cells and to $3x10^5$cell/ml for Dk RNAi$^{p18/pAZ0055}$ cells.

3.1.3. SDS PAGE and Western Blot

After the transfections, several clones for each of the RNAi constructs were tested by growth curves and Western blot analysis. Only one representing clone for each cell line is described here, in this thesis. These are the clones: PF RNAi$^{p18/p2T7\text{-}177}$ B2 clone, BF RNAi$^{p18/p2T7\text{-}177}$ C1 clone, Dk RNAi$^{p18/p2T7\text{-}177}$ B2 clone and Dk RNAi$^{p18/pAZ0055}$ A4 clone.

Noninduced cells and cells induced for 1, 2, 3 and 4 days were spun down (1300 g, 10 minutes, 4°C). In meantime, cell densities were counted and appropriate volumes of 1xPBS and 3xSDS loading dye were calculated to get ratio 2:1 and concentration $1x10^6$ cells/3 µl. Whole cell lysates were boiled at 97°C for 10 minutes and spun down (6000 rpm,

10 minutes, RT). Samples were then loaded on 12% SDS PAGE gel and run on 130 V for 2 hours.

For subsequent analysis, the proteins were blotted onto PVDF membrane (Thermo Scientific) and incubated overnight at PBS-T containing 5% milk. Next day the membranes were incubated with primary antibodies anti-ATPaseTb2 (1:2000 for PF cells, 1:1000 for BF cells, 1:1000 for Dk cells) (Šubrtová *et al*., 2015), anti-β (1:10000 for PF cells, 1:5000 for BF cells, 1:2000 for Dk cells $^{p18/p2T7\text{-}177}$, 1:5000 for Dk cells$^{p18/pAZ0055}$) and anti-p18 (1:2000 for PF cells, 1:1000 for BF and Dk cells) for 1 hour. Then, membranes were washed 3 times for 10 minutes in PBS-T, incubated with secondary antibodies (anti-rabbit goat IgG conjugated with horseradish peroxidase (HRP) (BioRad) for 1 hour, and again 3 times washed with PBS-T for 10 minutes. The signal was visualized using ClarityTM Western ECL Substrate (Biorad) in ChemidocTM MP instrument (Biorad).

Membranes for PF samples were then stripped with a stripping buffer in 50°C (30 minutes) and the membranes were processed as describe above with primary Hsp70 antibody (1:2000) and secondary anti-mouse goat antibody conjugated with HRP (BioRad).

3.1.4. Isolation of *T. brucei* mitochondria

Mitochondria were isolated by hypotonic lysis. Noninduced cells and cells induced for 1, 2, and 3 days in mid log phase (total number cells 1.5 x10^8 for BF cells and 2.5x10^8 for PF cells) were spun down (1300 g, 4°C, 10 minutes), resuspended in 1.5 ml of ice-cold NET and again spun down (1300 g, 4°C, 10 minutes). The cell pellets were resuspended in 1.4 ml of DTE and disrupted by passing through 25G needle. Immediately, 170 µl of 60% sucrose was added and samples were again spun down (15000 g, 10 minutes, 4°C). Pellets were resuspended in 500 µl of STM and 1.5 µl of 1 M $MgCl_2$ and 2.5 µl of 2.5 mg/ml DNAse were added to the cell suspension. Samples were incubated on ice for 1 hour. DNAse treatment was stopped by adding of 500 µl of cold STE and spun down (15000 g, 10 minutes, 4°C). Pellets were resuspended in 500 µl of STE, spun down and the washing step was repeated once again. The pelleted mitochondria were immediately used or they were kept in -80°C.

3.1.5. High resolution clear native electrophoresis

Isolated mitochondria from *T.brucei* PF RNAi^{p18} and BF RNAi^{p18} cells were resuspended in a digitonin lysis buffer (100 µl). The protein concentration was measured by a Bradford assays. The mitochondria were then spun down and resuspended in a digitonin

lysis buffer. The volume of the buffer depends on a protein concentration. The final concentration of protein sample was 1.6 mg/ml. The samples were lysed with digitonin at a ratio of 4 mg of digitonine to 1 mg of protein. Samples were incubated on ice for 1 hour and spun down (15000 g, 1 hour, 4°C). In the meantime, gradient native gels (3-12%) were poured manually. Again, the protein concentration of cleared supernatants was measured by a Bradford assay. Samples (10 μg or 20 μg depending on antibody) were loaded on the gel and left run in the 4°C at 90 V for 1 hour, then 130 V for 4 hours.

The proteins were blotted overnight onto nitrocellulose membrane (Life Sciences) in 4°C at 20 V. Next day, the membranes were processed as describe above with primary antibodies ATPaseTb2 (1:1000 for BF cells, 1:2000 for PF cells) and β (1:1000 for BF cells, 1:5000 for PF cells).

As a loading control, both BF mitochondria (2.5 μg) and PF mitochondria (5 μg) were loaded onto 12% SDS PAGE gel. The membranes were processed as describe above with primary antibodies Hsp70 (1:2000) and secondary antibody anti mouse goat IgG conjugated with HRP (1:2000, BioRad).

3.1.6. Measurement of Δψm

The Δψm was measured in PF, BF and Dk RNAi^{p18} cell lines. Cells were incubated at 27°C for PF cells or at 37°C in 5% CO_2 for Dk and BF cells. Noninduced and RNAi induced (for 1, 2, 3 and 4 days) cells were stained for 30 minutes with 60 nM tetramethylrhodamine ethyl ester (TMRE, Invitrogen). Trifluorocarbonylcyanide phenylhydrazone (FCCP, 20 μM) was used as a positive control. Stained cells were harvested (1300 g, 10 minutes, RT), resuspended in 1 ml of PBS and transferred into fluorescence-activated cell sorting (FACS) tubes. The cells were subsequently analyzed by the flow cytometr (BD FACS Canto II Instrument). Data were evaluated using BD FACSDiva (BD Company) software.

3.2. Drug treatment with JK-11 compound

We received this chemical compound from dr. Ulrike Holzgrabe from the University of Würzburg. The chemical formula of this compound is C24H23N3O9 and molecular weight is 497.45 g/mol.

3.2.1. Cell lines and growth

T. brucei PF427 strain was cultivated at 27°C in SDM-79 media with 10% FBS. *T.brucei* BF427 and dyskinetoplastic cells Dk164 were cultivated at 37°C in 5% CO_2 in HMI-9 with 10% FBS.

3.2.2. Screening for cytotoxicity by Alamar Blue assay

Chemical compound, JK-11, was tested in PF427, BF427 and Dk164 cells. PF427 cells ($1x10^5$ cells) or BF427 and Dk164 cells ($5x10^3$ cells), medium and inhibitor (Table 3.3) were used in a total volume of 200 µl per well. Cells were incubated for 72 hours in wet chambers at 27°C for PF427 cells or at 37°C in 5% CO_2 for BF427 and Dk164 cells. After incubation, resazurin solution (20 µl in concentration 1.25 mg/10 ml) was added and cells were incubated for additional 4 hours. The resulting fluorescence was read on the microplate reader (TECAN) using fluorescence excitation wavelength at 560 nm and reading emission at 590 nm. The results were analyzed by plotting the fluorescence intensity versus compound concentration using nonlineral regression (curve fit) and sigmoidal dose-response analysis by Graph Pad Prism software.

Tab. 3.3: Dilution series of JK-11 (from maximum to minimum).

JK-11 (concentration in µM)										
PF427	1000	500	250	125	62.5	31.25	15.6	7.8	3.9	1.95
BF427	200	100	50	25	12.5	6.25	3.125	1.56	0.78	0.39
Dk164	100	50	25	12.5	6.25	3.125	1.56	0.78	0.39	0.195

3.2.3. Measurement of Δψm in cells treated with JK-11

The mid log phase cells were incubated with appropriate drug concentration for 4 hours (at 27°C for PF427 cells or at 37°C+5% CO_2 for Dk164 and BF427 cell) and then processed for TMRE staining as decribed above.

3.2.4. Sumner ATPase assay with F_1-ATPase

Purified F_1-ATPase (kindly provided by Ondřej Gahura) (7 µl) was mixed with ATPase assay buffer to give a total volume 200 µl. Inbibitors were added to this mixture in the concentration range between 200 µM – 1 µM for JK-11. Azide (1 mM) was used as a positive control. DMSO, the solvent, was used to test to ensure that this chemical does not interfere with the reaction. The reaction was started by addition of 5 µl of ATP (200 mM) and was left incubated for 10 minutes at RT. The reaction was stopped by 4 µl of 70% perchloric acid. The mixture was quickly vortexed, left on ice for 30 minutes and spun down (16000 rpm, 4°C, 10 minutes). Supernatant (90 µl) was transferred to new eppi and developed with 500 µl of Sumner reagent buffer for 10 minutes in RT. The reaction

(200 µl) was then transferred into 96-well plate and its absorbance was measured at 610 nm on the microplate reader (TECAN).

3.2.5. Measurement of total mt ATPase activity using Sumner ATPase assay

The crude mitochondria from $1.5x10^8$ PF427 cells were washed once with 1 ml PBS-G and transferred to 1.5 ml eppi. The pellet was resuspended in 500 µl of SoTe buffer. SoTe buffer containing 0.03% digitonin (500 µl) was added into the mixture. The samples were left on ice for 5 minutes. Cell suspension was spun down (7000 rpm, 3 minutes, 4°C). The final pellet was resuspended in ATPase assay buffer (650 µl). The protein concentration was determined by a Bradford assay. Crude mitochondria (10 µg), various concentration of JK-11 inhibitor (250 – 12.5 µM) and ATPase assay buffer were mixed together in total volume of 100 µl. Azide (1 mM) and oligomycin (60 µM) were used as a positive controls. The mixture was pre-incubated for 10 minutes and the ATPase reaction was started by addition of 5 µl of ATP (100 mM). After 20 minutes, the reaction was stopped by 1.9 µl of 70% perchloric acid. The samples were processed as described above for F_1-ATPase Sumner assay.

For coupled reaction, JK-11 (250 µM) and azide (1 mM) or JK-11 (250 µM) and oligomycin (60 µM) were processed as described above.

3.2.6. ATP production in PF *T. brucei* mitochondria

By using *in vitro* ATP production assay, the ATP molecules produced by either substrate phosphorylation (SUBPHOS) or oxidative phosphorylation (OXPHOS) pathways can be measured. Succinate is used to trigger OXPHOS, while α-ketoglutarate is used as a substrate for SUBPHOS. In both pathways, ADP is imported via AAC to the matrix. Thus, atractyloside is used as an inhibitor of AAC for both pathways. In OXPHOS, electrons flow through complexes II – IV to pump protons into the matrix. F_oF_1-ATP synthase then uses this proton gradient to synthesizing ATP from ADP and Pi. Therefore, malonate, inhibitor of the complex II, is used to inhibit OXPHOS. On the other hands, SUBPHOS generates ATP from imported ADP by a reaction of the Krebs cycle (Besteiro *et al*., 2005). The produced ATP is then measured in a luciferase assay. The principle is shown in the scheme (Figure 3.4). Briefly, the ATP assay is based on the production of light caused by the reaction of ATP with luciferase and D-luciferin. The emitted light is proportional to the ATP concentration inside the cell.

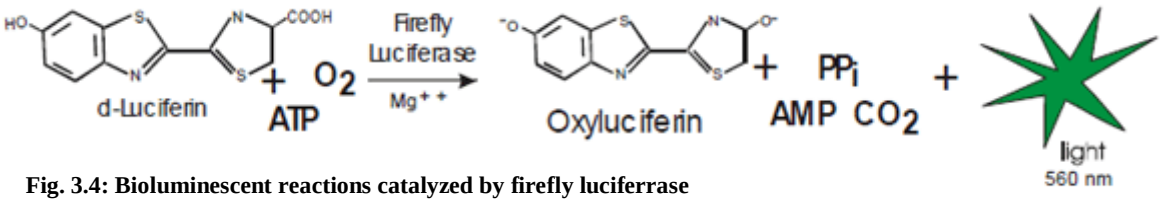

Fig. 3.4: Bioluminescent reactions catalyzed by firefly luciferrase
(http://www.biotek.com/resources/articles/luminescent-atp-concentrations.html).

Crude mitochondria were prepared as mentioned above. The organellar pellet was resuspended in 750 µl of ATP production buffer. The mixture (75 µl) was transferred to the new eppis and incubated for 10 minutes on ice with 1 µl of the tested inhibitor (JK-11 in various concentrations from 100 – 1.5625 µM). Atractyloside (47 µM) was used to inhibit the ATP/ADP carrier and and malonate (6.7 mM) was used to inhibit complex II. Succinate (5 mM) was added to trigger OXPHOS pathway, SUBPHOS pathway was triggered by α-ketoglutarate (5 mM). The reaction was started with ADP (67 µM) and left incubated in 27°C for 30 minutes. Reaction was stopped by addition of 1.5 µl of 70% perchloric acid, vortexed, and incubated for 10 minutes on ice. Samples were spun down (16000 rpm, 4°C, 10 minutes), The supernatants (60 µl) were mixed with 11.5 µl of 1 M KOH, incubated on ice for 10 minutes and spun down (10 minutes, 15000 rpm, 4°C). Supernatants (10 µl) were mixed with 40 µl of 0.5 M Tris-Acetate pH 7.75. The amount of ATP was measured at the Orion II adding 50 µl of luciferase solution (ATP bioluminiscence assay kit HSII, ROCHE).

3.3.List of used buffers and reagents

Agarose plate (1% NaCl, 1% peptone, 0.5% yeast extract, 1.5% agar)

ATPase assay buffer (0.2 M KCl, 10 mM Tris-HCl, 2 mM $MgCl_2$, pH 8.2).

ATP production buffer (20 mM Tris-HCl, 0.6 M sorbitol, 10 mM $MgSO_4$, 2.5 mg/ml fatty acid free BSA,15 mM KPi)

CytoMix buffer (25 mM HEPES pH 7.6, 120 mM KCl, 0.15 mM $CaCl_2$, 10 mM)

K_2HPO_4/KH_2PO_4 pH 7.6, (2 mM EDTA, 5 mM $MgCl_2$, 6 mM glucose)

Digitonin (0.2g/1 ml MilliQ)

Digitonin lysis buffer (2 mM ACA, 50 mM imidazole-HCl pH 7.0, 1 mM EDTA, 50 mM NaCl, pH 7.0)

DTE (1 mM Tris-HCl pH 8.0, 1 mM EDTA)

NET (0.15M NaCL, 0.1 M EDTA, 10 mM TRis-HCl pH 8.0)

PBS-G (5.6 mM $Na_2HPO_4x12H_2O$, 3.6 mM $NaH_2PO_4x2H_2O$, 0.145 M NaCl, 3.3 mM glucose)

PBS-T (5.6 mM $Na_2HPO_4x12H_2O$, 3.6 mM $NaH_2PO_4x2H_2O$, 0.145 M NaCl, 0.05% Tween)

Resazurin (1.25 mg/10 ml in 1xPBS pH 7.4)

SDS page loading dye (63 mM Tris Hcl, 10% Glycerol, 2% SDS, 0.0025% Bromophenol Blue, pH 6.8)

SOC medium (2% tryptone, 0.5% yeast extract, 10 mM NaCl, 2.5 mM KCl, 10 mM $MgCl_2$, 10 mM $MgSO_4$, 20 mM glucose)

SoTe buffer (0.6 M sorbitol, 20 mM Tris-HCl, pH 7.9, 2 mM EDTA)

STE (250 mM sucrose, 20 mM Tris pH 8.0, 10 mM EDTA)

STM (250 mM sucrose, 20 mM Tris pH 8.2, 2 mM $MgCl_2$)

Stripping buffer (6.25 mM Tris pH 6.8, 100 mM mercaptoethanol, 2% SDS)

Sumner reagent (8,8 g $FeSO_4x7H_20$ in 3,75 M sµlphuric acid adjusting volume with 900ml MilliQ and mixed with 6,6 g $(NH_4)_6Mo_7O_{24}x4H_2O$ in 100 ml MilliQ)

4. Results

4.1. The p18 subunit in *T. brucei*

Originally, the p18 subunit was considered to be a homolog of subunit b (Speijer *et al*., 1997). Recently, p18 was purified with F_1-ATPase in our laboratory (Gahura, manuscript in preparation). Our data suggested that p18 could be potentially subunit of F_1-ATPase. This is surprising observation taking into the consideration that composition of F_1-ATPase is extremely conserved. So far in all studied eukaryotic organisms, the F_1-part is composed of α, β, γ, δ, ε subunits and no additional subunits were ever identified in this catalytic moiety (Collinson *et al*., 1994; Velours and Arselin, 2000; Perez *et al*., 2014). Thus, identification of p18 as a bona fide subunit of F_1-ATPase might be first example of an exemption from this rule.

To determine if p18 is essential for growth of *T. brucei* cells and if it is important for activity and structural integrity of F_1-complex, we created RNAi cell line in which the expression of p18 can be silenced. Since the activity, function and role of F_oF_1-ATP synthase/ATPase differs between the *T. brucei* life stages, we silenced the expression of p18 in all three types of *T. brucei* cells available in our laboratory, namely in procyclic PF, bloodstream BF and dyskinetoplastic Dk *T. evansi* cells. A 452bp region of p18 gene was amplified and cloned either into head to head p2T7-177 vector or into stem loop vector pAZ0055. The RNAi linearized plasmids were transfected into 29-13 PF cells, SM BF cells and Dk cells *T. evansi*. After the antibiotic selection, the following clones were selected and thoroughly investigated: PF RNAi$^{p18/p2T7\text{-}177}$ B2 clone, BF RNAi$^{p18/p2T7\text{-}177}$ C1 clone, Dk RNAi$^{p18/p2T7\text{-}177}$ B2 clone and Dk RNAi$^{p18/pAZ0055}$ A4 clone.

4.1.1. RNAi^{p18} in PF and BF *T. brucei* cells

4.1.1.1. Growth curve of PF and BF RNAi$^{p18/p2T7\text{-}177}$ cells

To assess if p18 is important for *in vitro* growth of PF and BF *T. brucei* cells, the growth rate of RNAi non-induced (NON) and RNAi-induced (IND) cells was determined (10 days for PF cells or for 8 days for BF cells). Importantly, growth effect was observed at day 4 in PF cells (Figure 4.1) and at day 2 in BF cells (Figure 4.2) after RNAi induction.

In PF cells, silencing of p18 caused only a mild growth phenotype. It is noteworthy that the cells were cultivated in glucose-rich SDM-79 medium. In this medium, cells preferentially use glucose as a major source of ATP. Though pyruvate enters mitochondrion

and is converted to AcCoA, this molecule is not converted to citrate as one would expect, but it is metabolized to acetate. In this reaction a molecule of ATP is made by succinyl CoA synthetase. It is generally accepted that PF cells grown in high glucose concentration does not rely completely on oxidative phosphorylation (Coustou *et al*., 2008). Thus, an importance of F_oF_1-ATP synthase is decreased and observed growth phenotype is only mild.

In contrast to PF cells, a strong growth phenotype was observed 2nd day after RNAi induction in BF cells. At day 5, a subpopulation of RNAi resistant cells was no longer responsive to RNAi leading to the growth recovery of the culture. Probably, this recovery of growth was caused by powerful selection forces that act on these cells and miss a critical protein. This phenomenon is observed in BF cells very often (Chen *et al*., 2003). Nevertheless, the observed growth phenotype is in agreement with the essential function of F_oF_1-ATPase in BF trypanosomes. (Schnaufer *et al*., 2005; Brown *et al*., 2006).

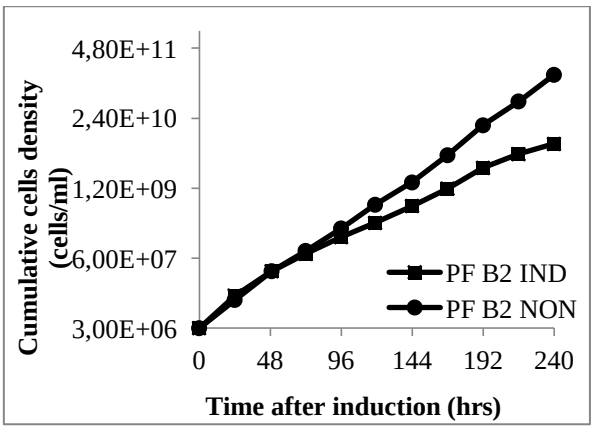

Fig. 4.2: Growth curve analysis of RNAi^{p18} in PF cells *T. brucei.*

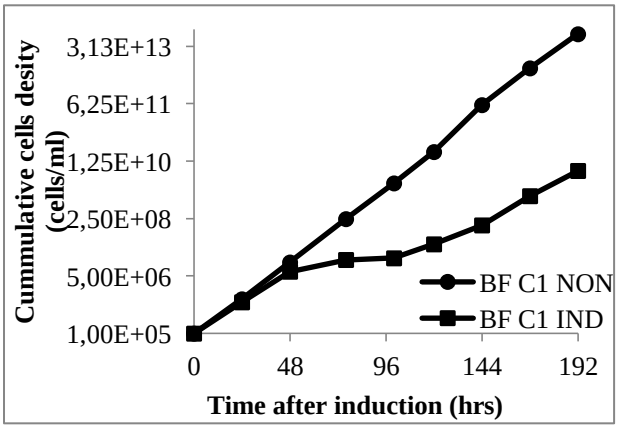

Fig. 4.2: Growth curve analysis of RNAi^{p18} in BF cells *T. brucei.*

4.1.1.2. Verification of PF and BF RNAi$^{p18/p2T7\text{-}177}$ cells using specific antibodies against p18, β and ATPaseTb2

The RNAi efficiency of PF and BF RNAi$^{p18/p2T7\text{-}177}$cell lines was confirmed by Western blot analysis using specific p18 antibody. Significant decrease of p18 abundance was observed at day 2 after RNAi induction in both PF (Figure 4.3) and BF (Figure 4.4) cells.

Since p18 is a novel subunit of F_1-ATPase we were also interested if other subunits of F_oF_1-complex might be affected upon p18 silencing. Indeed, both tested subunits (β and ATPaseTb2) showed a substantial reduction in their steady state abundance, suggesting that the stability of F_oF_1-ATPase is affected when p18 subunit is silenced (Figure 4.3 and 4.4).

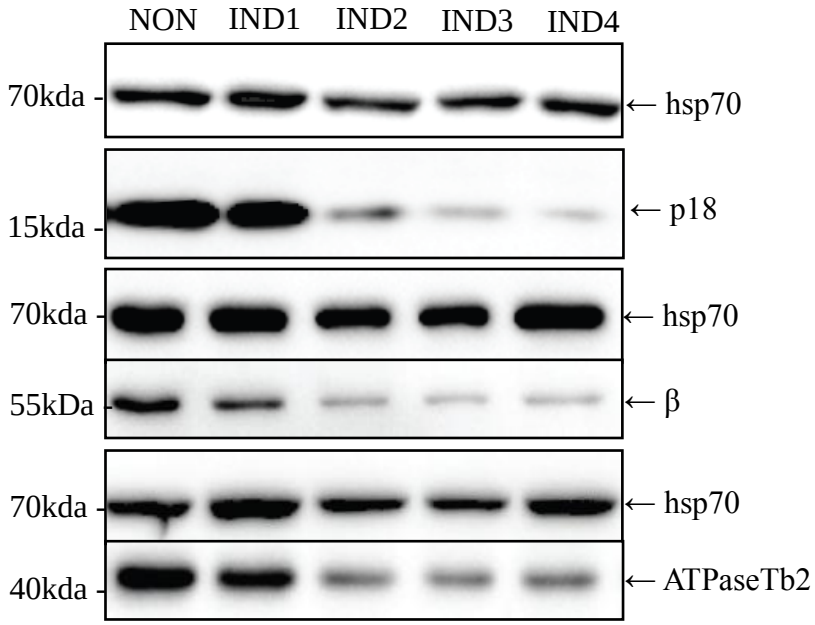

Fig. 4.3: Verification of RNAi^{p18} PF cells with p18, ATPaseTb2 and β specific antibodies. For subunit p18 (18kDa) were loaded 2.5x10^6 cells and used anti-p18 in 1:2000 dilution. For subunit β (55kDa): 1x10^6 cells, anti-β 1:10000. For subunit ATPaseTb2 (43kDa): 2.5x10^6 cells, anti-ATPaseTb2 1:2000. Sample marked as NON represents noninduced samples. Samples marked as IND1, IND2, IND3 and IND4 represent induced samples for 1, 2, 3 and 4 days. Upper panels serves as a control with Hsp70 (70kDa), the known mitochondrial marker.

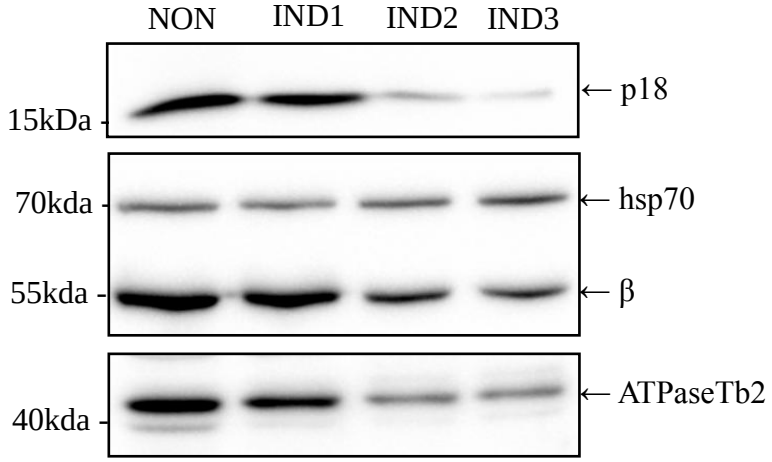

Fig. 4.4: Verification of RNAi p18 BF cells with p18, ATPaseTb2 and β specific antibodies. For subunit p18 (18kDa) were loaded 1x10^7 cells and used anti-p18 in 1:1000 dilution. For subunit β (55kDa): 1x10^6 cells, anti-β 1:5000. For subunit ATPaseTb2 (43kDa): 2.5x10^6 cells, anti-ATPaseTb2 1:1000. Sample marked as NON represents noninduced samples. Samples marked as IND1, IND2, IND3 and IND4 represent induced samples for 1, 2 and 3 days. Upper bands in β column serve as a control with Hsp70 (70kDa), the known mitochondrial marker. Membrane was processed with Hsp70 and then with anti-β antibody.

4.1.1.3. Structural integrity of F_1 and F_oF_1-complexes in RNAi^{p18} PF and BF cells

To reveal if the structural integrity F_oF_1-ATPase/synthase is affected upon p18 silencing, mt lysates from noninduced and RNAi induced cells were analysed by high resolution clear native electrophoresis followed by western blot analysis. Specific antibody against subunit β was used to detect F_1-ATPase, F_oF_1-monomer and dimer, while antibody

against subunit ATPaseTb2 was used to detect only the higher assemblies (monomer and dimer).

Importantly, upon p18 RNAi silencing, the RNAi^{p18} induced PF and BF cells showed a dramatic decrease of F_1 and F_oF_1-complexes indicating that p18 subunit is crucial for structural integrity of both, F_1-moiety and F_oF_1-complexes (Figure 4.5 and 4.6). The mt lysates were also analyzed by SDS PAGE followed by western blot analysis using anti-hsp70 antibody to show equal protein content in the studied samples.

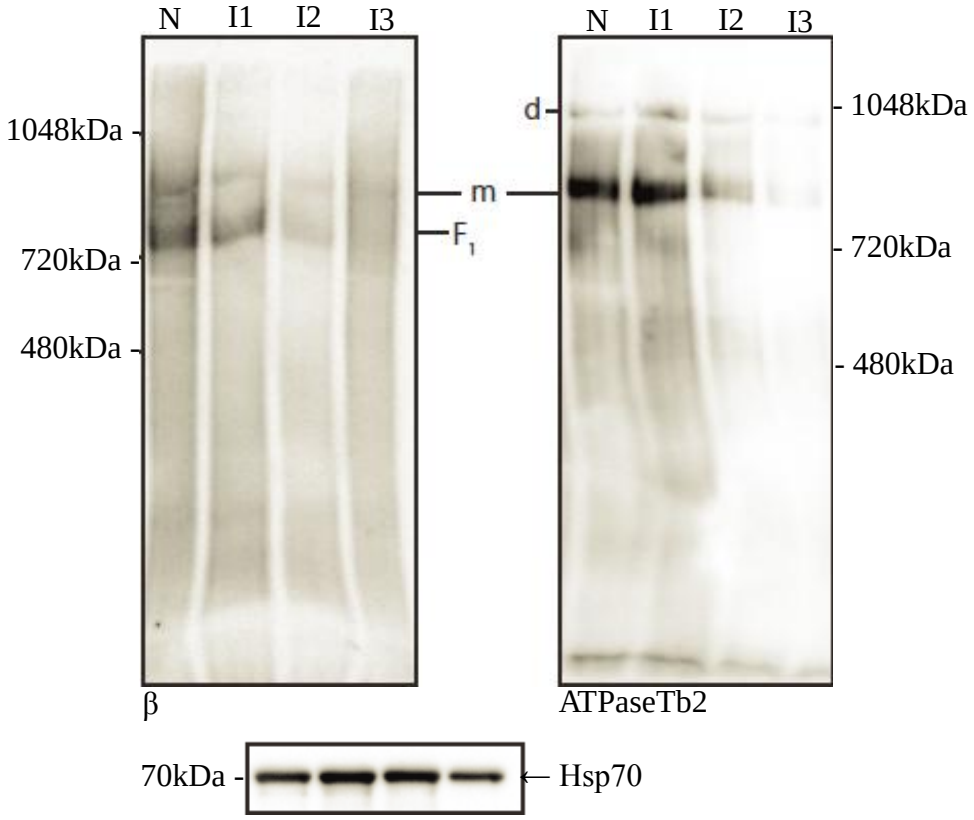

Fig. 4.5: The structural integrity of F_oF_1 ATP synthase in RNAi^{p18} PF cells. F_1 is F_1-ATPase, m is monomer and d is dimer F_oF_1-ATP synthase. For ATPaseTb2 1:2000 and β 1:5000 were used 20 µg of proteins. As a control for Hsp70 antibody 1:2000 were used 5 µg of proteins. Sample marked as N represents noninduced samples. Samples marked as I1, I2 and I3 represent induced samples for 1, 2 and 3 days.

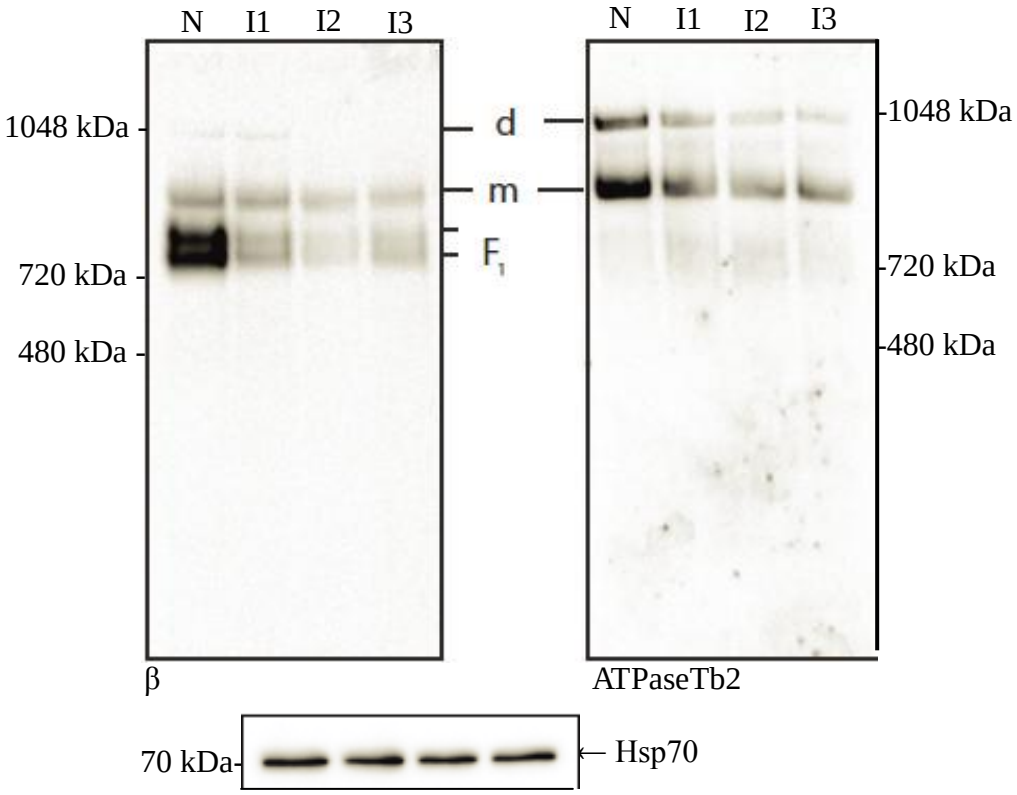

Fig. 4.6: The structural integrity of F_oF_1 ATPase in RNAi^{p18} BF cells. F_1 is F_1-ATPase, m is monomer and d is dimer F_oF_1-ATP synthase. For ATPaseTb2 1:1000 and β 1:2000 were used 10 µg of proteins. As a control for Hsp70 antibody 1:2000 were used 2.5 µg of proteins. Sample marked as N represents noninduced samples. Samples marked as I1, I2 and I3 represent induced samples for 1, 2 and 3 days.

4.1.1.4. Changes in Δψm in RNAi^{p18} PF and BF cells

To address if the Δψm is affected in PF and BF RNAi$^{p18/p2T7\text{-}177}$ cells, it was measured in PF and BF noninduced and RNAi induced cells. In BF cells, the Δψm is maintained by the hydrolytic activity of F_oF_1-ATPase followed by proton translocation through the mt inner membrane. (Schnaufer *et al.*, 2005). On the other hand, in PF cells, the Δψm is maintained by convential proton-pumping activities of complexes III and IV (Besteiro *et al.*, 2005). This proton motive force is then used by F_oF_1-ATP synthase to produce ATP by oxidative phosphorylation. Thus, if F_oF_1-ATP synthase/ATPase function is affected, one would expect a build-up of Δψm in PF cells, as the protons are not allowed to come back to matrix and they accumulate in the inner membrane space, while in BF cells the Δψm should be significantly decreased.

The Δψm was measured with a fluorescent dye TMRE by flow cytometry. Fluorescent intensity measured in non-induced cells was set as 100%. FCCP, an uncoupler, was used as a positive control. PF cells induced for 1, 2, 3 and 4 days showed higher Δψm compared to non-induced cells (Figure 4.7). This observation is in agreement with the proposed function of PF mitochondrion and indirectly demonstrates that the function of the F_oF_1-ATP synthase complex is disturbed. On the other hand, BF cells

induced for 1, 2 and 3 days showed lower Δψm compared to non-induced cells (Figure 4.8). Again, this observation is in agreement with the proposed function of BF mitochondrion and indirectly demonstrates that function of the F_oF_1-ATPase complex is disrupted.

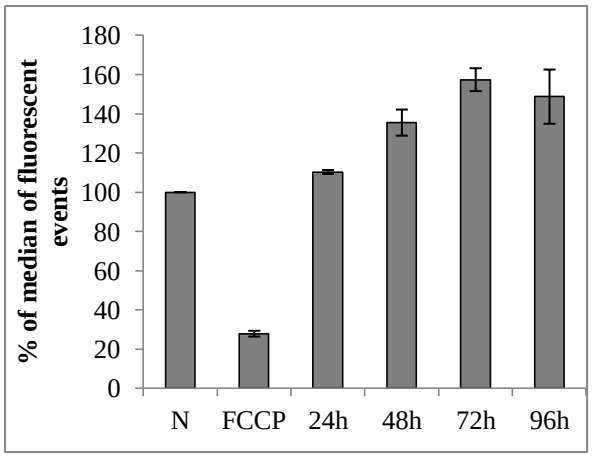

Fig.4.7: The Δψm in RNAi^{p18} PF cells.

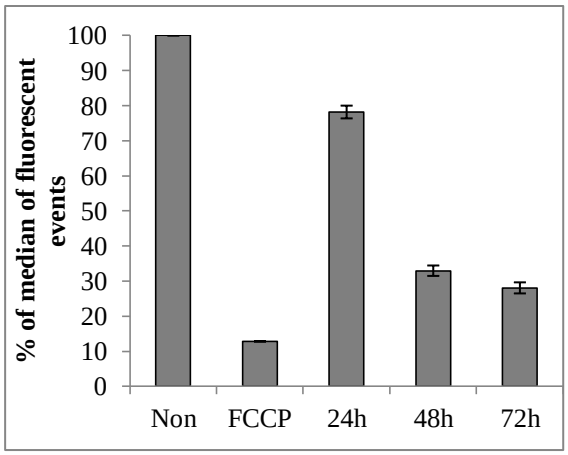

Fig.4.8: The Δψm in RNAi^{p18} BF cells.

4.1.2. RNAi^{p18} in Dk *T. evansi* cells – p2T7-177 vector versus pAZ0055

Dyskinetoplastic cells lost all or critical parts of their kDNA and they lack mitochondrial encoded genes (Schnaufer *et al*., 2002). Thus, it was thought that the ATPase is composed only from F_1-moiety. Recent data shows, that a minor fraction of F_1-ATPase is still associaeted with F_o-moiety and is located near to the mitochondrial inner membrane (Šubrtová *et al*., 2015). Whilst, the Dk F_oF_1-ATPase does not possess a proton pore, the Δψm is kept by hydrolytic activity ofthe F_1-ATPase coupled with the electrogenic exchange of ATP^{3-} for ATP^{4-} by AAC (Schnaufer *et al*., 2005). Interestingly, Dk trypanosomes involved compensatory mutations in the nuclearly encoded F_1 subunit γ allowing them to survive the loss of mt genome. These mutations (e.g. L262P or A273P), can result in increased ATPase activity (Dean *et al*., 2013). Since the composition and role of the F_oF_1-ATPase is different in Dk cells, it would be interesting to examine the importance of p18 subunit in these trypanosomes.

4.1.2.1. Growth curve analysis of RNAi$^{p18/p2T7\text{-}177}$ and RNAi$^{p18/pAZ0055}$ Dk cells

To consider if p18 is important for *in vitro* growth of DK *T. evansi* cells, the growth rate of RNAi non-induced (NON) and RNAi-induced (IND) cells was determined for 9 days for both Dk cell clones. Surprisingly, neither in RNAi$^{p18/p2T7\text{-}177}$ clone B2 (Figure 4.9) nor in RNAi$^{p18/pAZ0055}$clone A4 (Figure 4.10) the growth phenotype was observed. This result was quite surprising as it may suggest that p18 is not essential for Dk trypanosomes and thus its function differs dramatically compared to PF and BF trypanosomes.

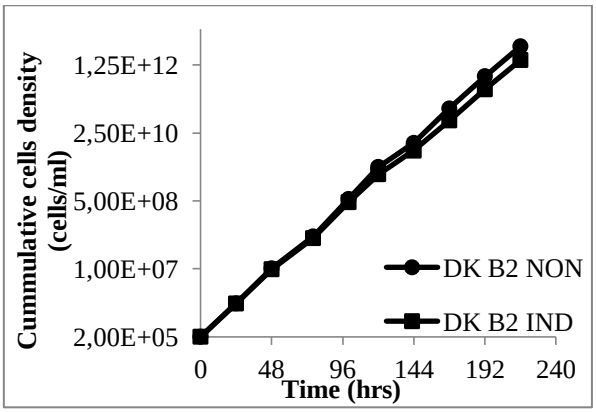

Fig. 4.9: Growth curve analysis of RNAi$^{p18/p2T7-177}$ DK B2.

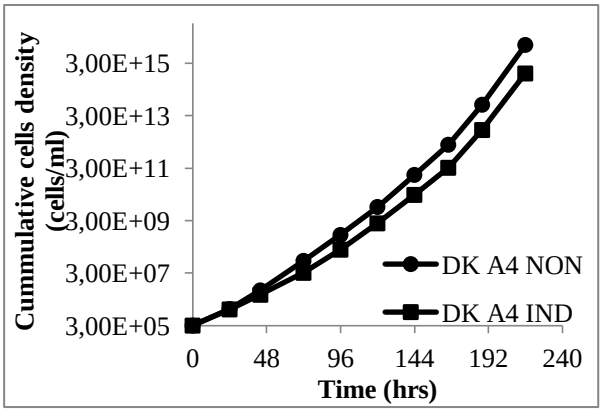

Fig. 4.10: Growth curve analysis of RNAi$^{p18/pAZ0055}$ DK A4.

4.1.2.2. Verification of Dk RNAi$^{p18/p2T7-177}$ and RNAi$^{p18/pAZ0055}$ cells using specific antibodies against p18, β and ATPaseTb2

The efficiency of RNAi knock down of p18 in both cell line clones was confirmed by Western blot analysis using specific p18 antibody. Significant decrease of p18 steady state abundance was observed at day 2 after RNAi induction in both RNAi$^{p18/p2T7-177}$ B2 clone (Figure 4.11) and RNAi$^{p18/pAZ0055}$ A4 clone (Figure 4.12). Even if a small fraction of the protein was always detected, this result would suggest that p18 is not essential for Dk cells and it is not important for the integrity of F_1-moiety.

To test if other subunits of Dk F_oF_1-ATPase (subunits β and ATPaseTb2) are affected upon p18 RNAi, the RNAi non-induced and induced protein samples were also tested with antibodies against subunit β and ATPaseTb2. In a case of Dk RNAi$^{p18/p2T7-177}$, a slight decrease were observed for all tested subunits, however decrease steady state abundance was also detected for unspecific protein bands at day 4 post induction (Figure 4.11). This would suggest that in this sample there were less protein in general or the proteins were unspecifically degraded. Nevertheles, no changes were observed in RNAi$^{p18/pAZ0055}$ implying that the steady state abundance of the two studied subunits (β and ATPaseTb2) is not affected.

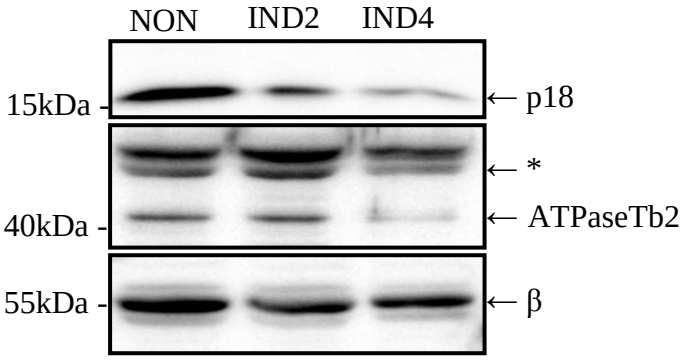

Fig. 4.11: Verification of RNAi$^{p18/p2T7-177}$ Dk cells with p18, ATPaseTb2 and β specific antibodies. For subunit p18 (18kDa) were loaded 1x10^7 cells and used anti-p18 in 1:1000. For subunit β (55kDa): 2.5x10^6 cells, anti-β 1:2000. For subunit ATPaseTb2 (43kDa): 2.5x10^6 cells, anti-ATPaseTb2 1:1000. Sample marked as NON represents noninduced samples. Samples marked as IND2 and IND4 represent induced samples for 2 and 4 days. * represents unspecific bands.

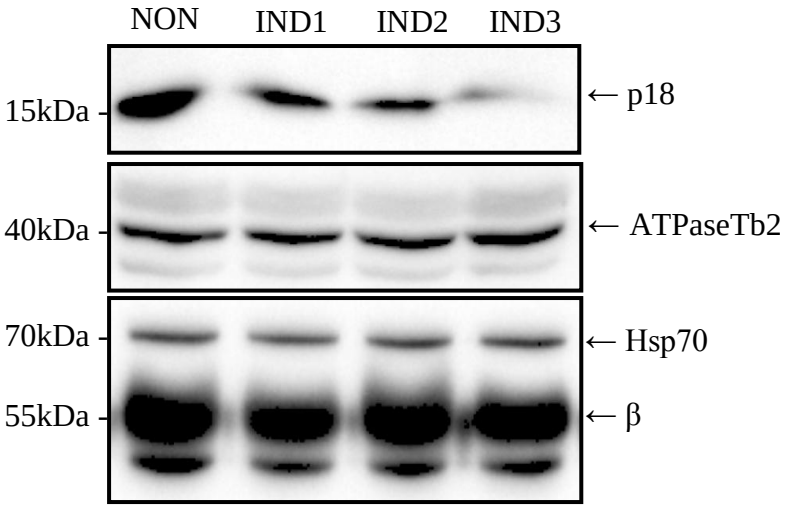

Fig. 4.12: Verification of RNAi$^{p18/pAZ0055}$ Dk cells with p18, ATPaseTb2 and β specific antibodies. For subunit p18 (18kDa) were loaded 1x10^7 cells and used anti-p18 in 1:1000 dilution. For subunit β (55kDa): 1x10^6 cells, anti-β 1:5000. For subunit ATPaseTb2 (43kDa): 2.5x10^6 cells, anti-ATPaseTb2 1:1000. Sample marked as NON represents noninduced samples. Samples marked as IND1, IND2 and IND3 represent induced samples for 1, 2 and 3 days. Upper bands in β column serve as a control with Hsp70 (70kDa), the known mitochondrial marker.

4.1.2.3. Changes in Δψm in Dk RNAi$^{p18/p2T7-177}$ and RNAi$^{p18/pAZ0055}$ cells

Even if the western blot analysis did not show a significant decrease in the catalytic subunit β, we decided to test if the Δψm is affected in the RNAi induced cells. The Δψm was measured with a fluorescent dye TMRE by flow cytometry. Fluorescent intensity measured in non-induced cells was set as 100%. FCCP, an uncoupler, was used as a positive control. The Δψm was slightly affected in both clones of RNAi cell lines. In the clone RNAi$^{p18/p2T7-177}$ B2 (Figure 4.13), the Δψm was reduced by 33 % at day 3 and by 40% at day 4 after RNAi induction. In the clone RNAi$^{p18/pAZ0055}$ A4 (Figure 4.14), the Δψm was slightly reduced at day 2 day by 20% after RNAi induction and stayed reduced by 30 % until day 4. Although we measured a decreased Δψm, we didn´t observed any growth phenotype. Thus, the function of F_1-ATPase seems to be not optimal, however this complex is capable to maintain the Δψm at the level that does not cause a growth phenotype.

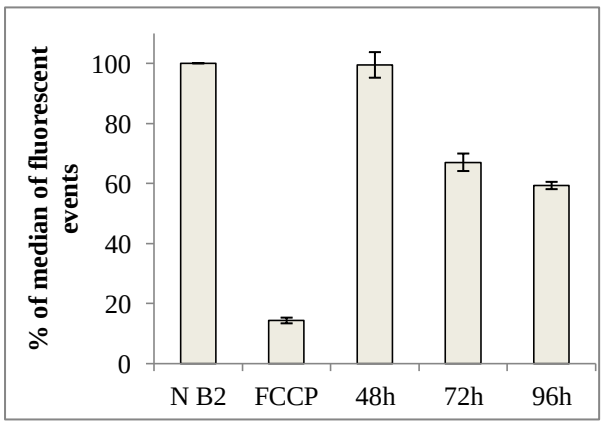

Fig. 4.13: The Δψm in RNAi$^{p18/p2T7-177}$ clone B2.

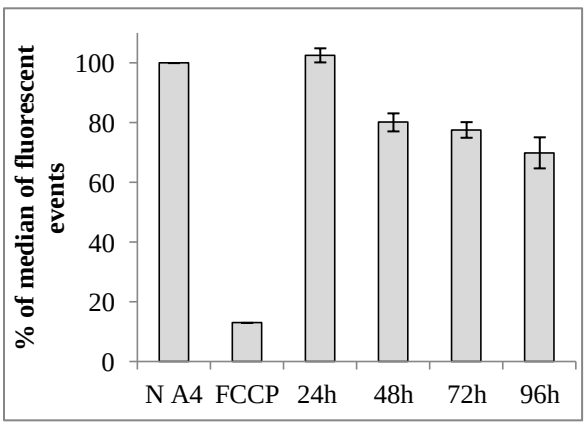

Fig. 4.14: The Δψm in RNAi$^{p18/pAZ0055}$ clone A4.

4.2. JK-11 in trypanosomatids

JK-11 is a potential drug that was developed to interfere with the hypusine synthesis in parasitic protists (Goebel *et al*., 2008). Interestingly, first phenotypic analyses showed that this drug also affect the $\Delta\psi m$ in BF cells. This observation raised a question if this compound does not affect activity of the F_oF_1-ATPase complex. In order to examine this possibility, we performed several assays to assess JK-11 inhibition of *T. brucei* mitochondrion function.

4.2.1. Cytotoxicity of JK-11 in PF, BF and DK cells

The cytotoxicity of the selected compound JK11 was determined by Alamar blue assay (Räz *et al*., 1997). The cells were incubated with the different concentrations of JK-11 for 72 hours followed by 4 hours incubation wirh resazurin. The EC_{50} values for each cell type were calculated by GraphPad Prism software (Table 4.1.) from the dose-response data (Figure 4.15, 4.16 and 4.17).

Interestingly, we observed a small variation in JK-11 cytotoxicity for the different trypanosome cell types. JK-11 affect the Dk cells the most, as the EC_{50} values were 7.8±0.2 µM. The EC_{50} values were a little bit higher for BF cells (12.7±3.7 µM). The PF cells were the least sensitive to JK-11 treatment, however still quite toxic as the EC_{50} values reached 17.7±5.2 µM.

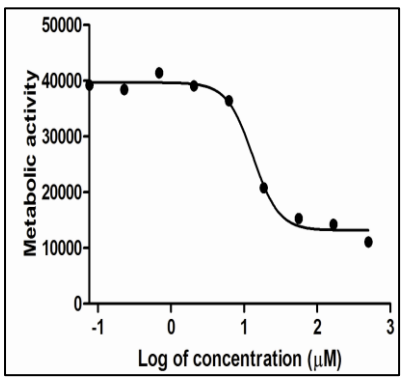

Fig. 4.15: Action of JK-11 in PF cells.

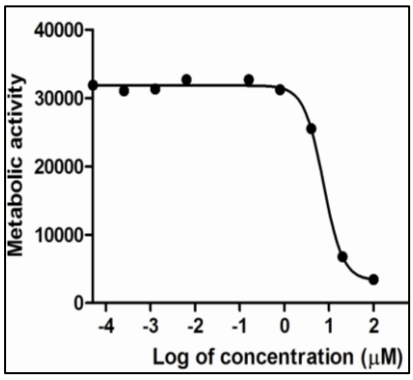

Fig. 4.16: Action of JK-11 in BF cells.

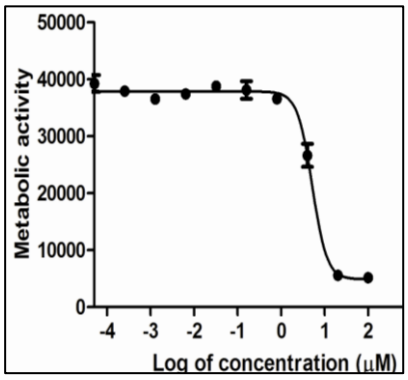

Fig. 4.17: Action of JK-11 in K cells.

Tab. 4.1: List of EC_{50} values for JK-11.

Type of cells	EC_{50} (µM)
PF427 cells	17.7±5.2
BF427 cells	12.7±3.7
Dk164 cells	7.8±0.2

4.2.2. Changes of ψm in PF, BF and Dk cells

Pilot experiments with JK-11 compound showed that this compound may affect the Δψm in BF cells (personal communication, Heike Bruhn). In order to reproduce these results, we decided to test different concentrations of JK-11 in PF, BF and Dk cells. These cells were pre-treated with JK-11 compound for 4 hours and then Δψm was measured using TMRE dye and flow cytometry. Interestingly, no changes in Δψm were observed in PF cells (Figure 4.18), while BF (Figure 4.19) and Dk (Figure 4.20) cell were affected when higher concentrations of JK-11 were used. In a case of BF cells, 3 times higher concentration than the EC_{50} value diminished Δψm almost completely. Dk cells seem to be more sensitive to JK-11 treatment, as 20 μM of JK-11 fully reduced the Δψm.

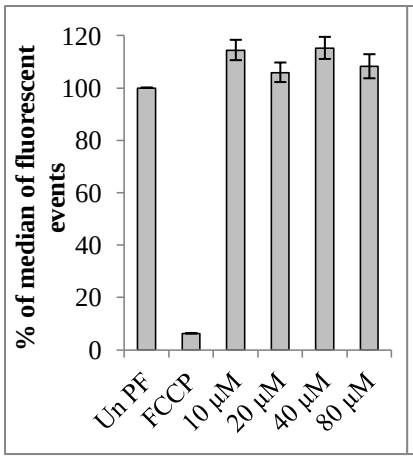

Fig. 4.18: The Δψm in PF cells.

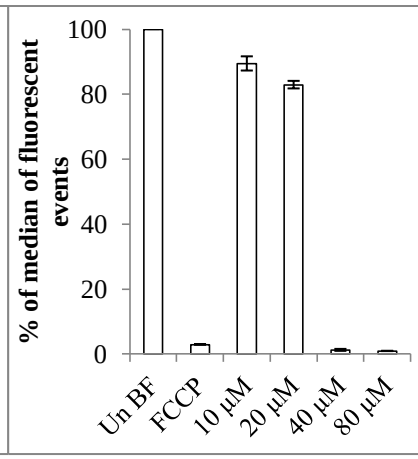

Fig. 4.19: The Δψm in BF cells.

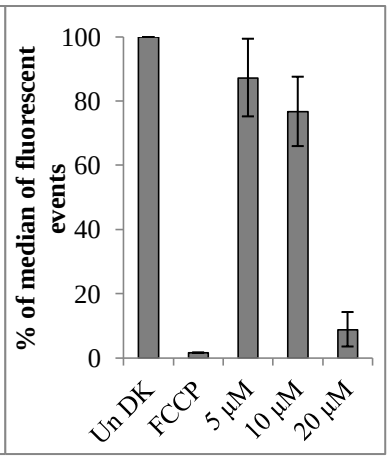

Fig. 4.20: The Δψm in Dk cells.

Since no effect was observed for PF cells, while a robust effect of JK-11 treatment on the Δψm was detected in BF and DK cells, these results suggest that indeed JK-11 may affect the hydrolytic activity of F_oF_1-ATPase.

4.2.3. Hydrolytic activity of F_1-ATPase by Sumner ATPase assay

To test if JK-11 inhibits that hydrolytic activity of F_oF_1-ATPase complex, we employed a Sumner ATPase assay. It is sensitive and fast method to determine hydrolysis of ATP by detecting inorganic phosphate that is realesed upon ATP hydrolysis (Law *et al*., 1995). First, we determined the hydrolytic activity of a purified F_1-ATPase from PF *T. brucei* (Figure 4.21). Assay was done in triplicates and values are expressed in %. Surprisingly, in contrast to Δψm measurements, specific activity of F_1-ATPase seems to be unaffected by 200 μM of JK-11. Azide (1 mM) served as a positive control as it inhibits the F_1-ATPase. DMSO served as a negative control, to exclude any possible interference of the JK-11 solvent.

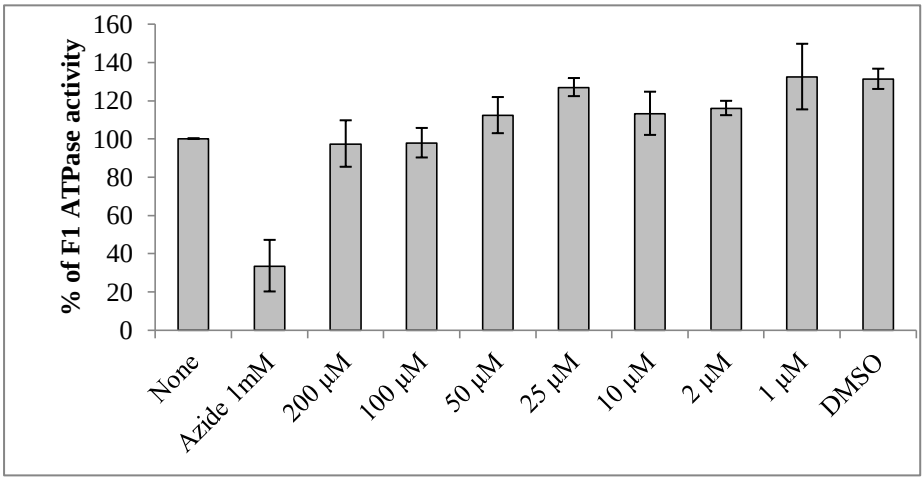

Fig. 4.21: The specific ATPase activity of F1-ATPase with JK-11 treatment.

4.2.4. Hydrolytic activity of F_oF_1-ATPase by Sumner ATPase assay

Since the compound JK-11 was not active against the purified F_1-complex, we then tested if it can inhibit the hydrolytic activity of fully assembled F_oF_1-complex in crude mitochondria. First we prepared crude mitochondrial enriched fractions from PF *T. brucei* and measured the activity of F_oF_1-ATPase when treated with various concentrations of JK-11 (Figure 4.22). Since there are other ATPases in these samples, the lysates were treated with the specific F_1-ATPase inhibitor, azide and F_oF_1-inhibitor, oligomycin (Lardy *et al*., 1975; Bowler *et al*., 2006). Importantly, increasing concentrations of JK-11 approached the same inhibition as the azide and oligomycin control, albeit at much higher concentrations than its measured EC_{50}.

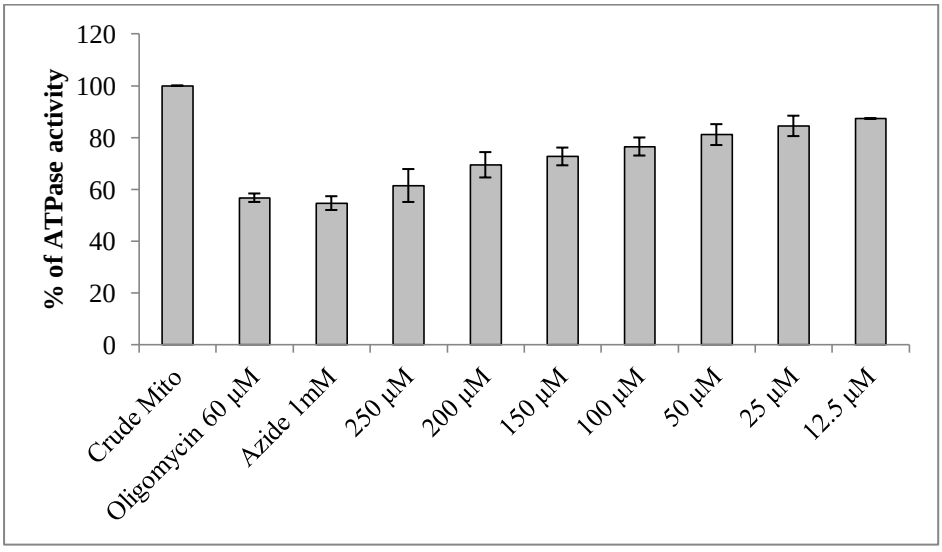

Fig. 4.22: The specific ATPase activity of FoF1-ATPase with JK-11 treatment.

Importantly, the same level of inhibition was detected when the crude mitochondria were treated with both oligomycin and JK-11 at the same time indicating that both inhibitors are acting on the same target, F_oF_1-ATPase (Figure 4.23). Interestingly, bigger inhibition was

detected when the crude mitochondria were treated with azide and JK-11 inhibitors, suggesting that JK-11 acts on a fully assembled F_oF_1-complex.

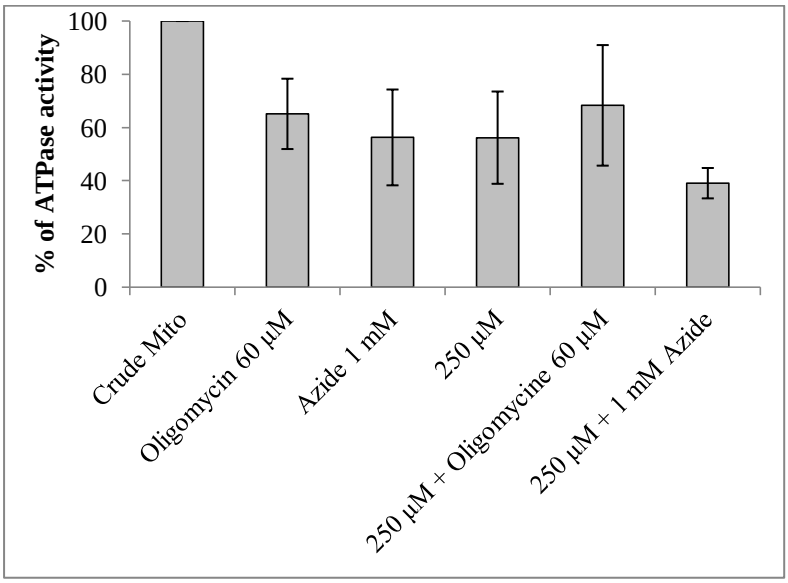

Fig. 4.23: Hydrolytic activity of F_oF_1-ATPase in coupled reactions.

4.2.5. ATP production of F_oF_1-ATP synthase

We established that JK-11 inhibits the hydrolytic activity of F_oF_1-ATPase and now we were interested if this compound also interferes with the forward activity of this complex. For this purpose we employed ATP production assay to measure ATP produces by oxidative phosphorylation in the purified crude mitochondria. For this reaction, (Figure 4.24), succinate was used as a substrate. Malonate, a specific inhibitor of complex II (succinate dehydrogenase), reduced the ATP production down to 5.7% of untreated sample. Atractyloside, a specific inhibitor of ATP/ADP carrier, also reduced ATP production to 12.7%. Interestingly, JK-11 at the concentration of 100 µM reduced production of ATP by 86%. At lower JK-11 concentration, the ATP production by oxphos was also affected, being reduced by ~40% when 1.5625 µM of JK-11 was used.

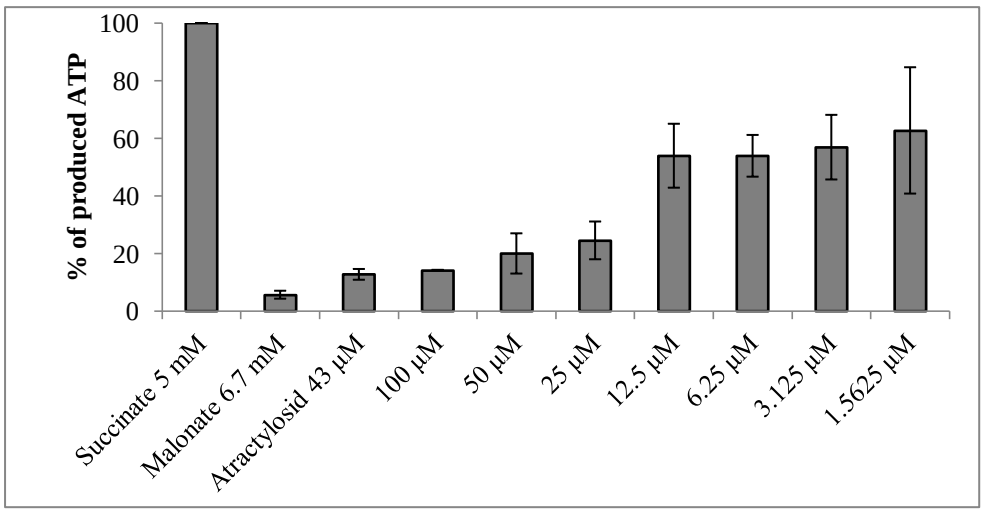

Fig. 4.24: ATP production - OXPHOS with JK-11 treatment.

To ensure that JK-11 does not affect any ATP producing reactions, we also investigated the ATP production by a substrate phosphorylation pathway. In this case, (Figure 4.25) the substrate phosphorylation pathway was triggered by α-ketoglutarate and atractyloside served as a positive control as it inhibits the ADP import to mitochondrion. Importantly, there was no significant decrease in ATP production upon a treatment with JK-11 even at the highest concentrations used.

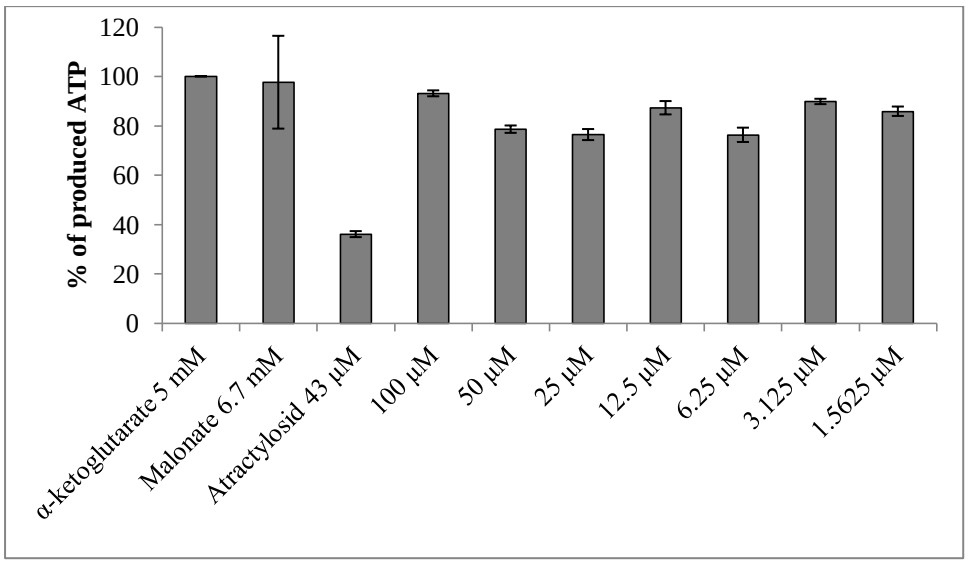

Fig. 4.25: ATP production - SUBPHOS with JK-11 treatment.

5. Discussion

5.1. Novel F_1-ATPase subunit p18

F_oF_1-ATP synthase is a remarkable molecular nanomotor responsible for the synthesis of the majority cellular ATP in the living cell (Boyer, 1997). This molecular machine consists of two parts – F_1-ATPase and F_o-ATPase. Both parts are linked together by a central and a peripheral stalk (Walker and Dickson, 2006; von Ballmoos *et al*., 2008). Composition of F_1-moiety seems to be strictly conserved as in all model eukaryotes studied so far, this subcomplex is composed of subunits α, β, γ, δ and ε (Collinson *et al*., 1994; Velours and Arselin, 2000). In contrast to conserved F_1-moiety, the F_o-part usually contains additional subunits, which are species/clade specific. Recently, studies of non-model organisms revealed possible significant differences of the mitochondrial F_oF_1-ATP synthase between different eukaryotic groups. Mainly, some subunits are missing. For example, in apicomplexan parasite *Plasmodium falciparum* and in free-living ciliate *Tetrahymena thermophila*, the subunits a, b, d and F6 are missing in their ATP synthase (Balabaskaran *et al*., 2010; Praveen Balabaskaran *et al*., 2011). In another organisms, such as green alga *Euglena gracilis* (Perez *et al*., 2014) or chlorophycean algae *Chlamydomonas* and *Polytomella* (Cardol *et al*., 2005; van Lis *et al*., 2007), the subunit b, d, and A6L were not identified. In addition to missing subunits, severel new components were identified in *T. thermophila* and *Polytomella*. In *T. thermophila*, the Ymf66 have been identified. This extremely divergent mitochondrially encoded protein is proposed to replace the subunit a of F_o-part (Balabaskaran *et al*., 2010). In *Polytomella*, several novel ATP synthase associated proteins (ASA1-9) have been recognized probably forming the building blocks of the peripheral stalk (Vázquez-Acevedo *et al*., 2006). Together, these studies uncovered the remarkable differences in composition of the ATP synthase complexes between these non-traditional and traditional (*S. cerevisiae* and *B. taurus*) model organisms. Although significant differences in F_o-moiety were presented in these organisms, any alterations have never been identified in the composition of their F_1-moiety.

T. brucei F_oF_1-ATPase/ATP synthase is composed of typical F_1-moiety subunits (α, β, γ, δ, and ε) and the F_o subunits (OSCP, a, c). In addition to these well known subunits, the parasite´s complex also contains 14 subunits (Zíková *et al*., 2009) with no homology outside Kinetoplastida or Euglenozoa (Perez at el., 2014). One such subunit (ATPaseTb2) was recently characterized in details and its function within the peripheral stalk was suggested (Šubrtová *et al*., 2015). Importantly, an additional protein, p18, was identified in F_1-ATPase

purifications implying that this protein might be a novel F_1-subunit (Gahura, manuscript in preparation).

In Kinetoplastids, the p18 subunit is encoded by a nuclear genome and its protein product (gene ID in TritrypDB is Tb927.5.1710) is localized in the mitochondrion (Bringaud *et al*., 1995). This protein was originally assigned to F_o-moiety based on a very low homology of *L. tarentolae* p18 with *E. coli* and *B. taurus* subunit b as only 6 amino acids on the C-terminal sequence (Speijer *et al*., 1997). Although supposed F_o-ATPase association, the p18 subunit was partially co-purified with F_1-ATPase in *L. tarentolae* (Nelson *et al*., 2004). In another study, p18 was silenced in PF cells *T. brucei* (Hashimi *et al*., 2010) and the reduced abundance of F_oF_1-ATP synthase complexes suggested that p18 may play a significant role in the integrity of F_oF_1-ATP synthase. Recently in our laboratory, p18 was co-purified with F_1-ATPase (Gahura, manuscript in preparation). Since p18 was originally considered to be a subunit of F_o-moiety, we decided to analyse its possible role in F_1-moiety structural integrity and enzymatic function. Because the role and activity of F_oF_1-ATPase/ATP synthase differs during life cycle stages of *T. brucei*, we have generated RNAi cell lines in all three available trypanosome cell types; PF, BF and Dk cells.

Our data suggests, that p18 is important for growth of PF cells and crucial for BF cells. In BF cells, this observation is in agreement with the essential function of F_oF_1-ATPase in this life stage as this complex hydrolyzes ATP to generate $\Delta\psi m$ (Schnaufer *et al*., 2005; Brown *et al*., 2006). In case of PF cells grown in glucose-rich medium SDM-79, the importance of F_oF_1-ATP synthase is reduced and observed phenotype was only mild. Most likely, if we would use the glucose-depleted medium SDM-80, these growing conditions would lead to amino acid catabolism followed by ATP generation by OXPHOS (Coustou *et al*., 2008). Thus, presumably, the observed growth phenotype would be stronger. Importantly, the stability of the F_1-moiety was strongly affected in both PF and BF RNAi^{p18} induced cells suggesting that p18 subunit is critical for F_1-ATPase structural integrity. As expected, the $\Delta\psi m$ was increased in PF cells while significantly decreased in BF cells in the absence of p18.

To generate p18 RNAi Dk cell line, we originally used the head-to-head T7 promoters p2T7 177 vector, since the same vector was used successfully to generate PF and BF RNAi^{p18} cell lines. Unexpectedly, none of the obtained Dk cell lines showed growth phenotype. The steady state abundance of p18 in RNAi induced cells was significantly reduced compared to non induced cells. Furthermore, the $\Delta\psi m$ was also decreased, although

only by 40% at day 4 upon tetracyclin induction. The observed phenotypes can be explained in two different ways. First, p18 is not essential and its role is dispensable for Dk cells. Second, the efficiency of the RNAi induction was not high enough to eliminate the protein completely and thus reveal the growth phenotype. To improve the RNAi efficienty, p18 RNAi fragment was cloned into a stem loop vector. After the selection process, which took longer than usually, only one cell line was recovered. When the cell line was growing regularly, the RNAi was induced by tetracycline addition into the media. Again, no growth phenotype was observed over the 10 days period, steady state abundance was significantly decreased and the $\Delta\psi m$ was reduced by 30% at day 4 post-induction. Thus, when p18 is silenced, the hydrolytic function of F_1-ATPase is not optimal, but the hydrolytic rate is at the satisfactory level to maintain $\Delta\psi m$ at the level that does not cause a growth phenotype. To understand the function of p18 in Dk cells in more details, a knock out cell line would have to be generated.

In conclusion, our data suggest that p18 is novel *bona fide* subunit of F_1-ATPase in PF and BF trypanosome cells. This proposal breaks the long-standing conception of the strict conservancy of the F_1-ATPase complex in eukaryotes.

5.2. Mode of action of JK-11

The 4-oxopiperidone-3,5-dicarboxylates inhibit polyamine biosynthesis at a various parasitic organisms namely *Plasmodium falciparum*, *Leishmania major* and *Trypanosoma brucei brucei* (Goebel *et al*., 2008). One of these compounds, JK-11, was investigated for its potential to inhibit mitochondrial fundemantal functions. The preliminary data showed that this compound affects the $\Delta\psi m$ generated by F_oF_1-ATPase in BF cells. Therefore, we decided to get the better insight into the mode of action of JK-11.

The EC_{50} values of JK-11 in BF427, PF427, and Dk164 cells showed, that JK-11 is the most potent inhibitor of Dk cells, then BF cells and finally PF cells. With the known EC_{50} values the measurements of the $\Delta\psi m$ were repeated. The $\Delta\psi m$ was increased in PF cells but decreased in BF and Dk cells. This observation supports theory, that JK-11 affects the function of F_oF_1-ATP synthase/ATPase.

Since the purification of *T. brucei* F_1-ATPase is routinely performed in our laboratory, we decided to measure the effect of JK-11 on its reversed hydrolytic activity first. Interestingly, we didn´t observe any inhibition of the F_1-ATPase hydrolytic activity. Thus, we concluded that the JK-11 is not acting on a free F_1-ATPase. Therefore, we were curious

if JK-11 affects hydrolytic activity of the fully assembled F_oF_1-complex. We observed 40% reduction in F_oF_1-ATPase activity when cells were treated with 250 µM JK-11. In comparison to azide and oligomycin, both these inhibitors reduced the total ATPase activity by 45%. To ensure that JK-11 affects only F_oF_1-ATPase, we incubated crude mitochondria with JK-11 and either azide or oligomycin at the same time. Inhibition of the coupled reactions evinced the similar inhibition as inhibition with azide or oligomycin. Therefore, both JK-11 and specific inhibitors target only F_oF_1-ATPase and not any other ATPases.

To determine if JK-11 affects forward function of F_oF_1-ATP synthase, the synthesis of ATP, the ATP production was measured. This reaction is measuring the activity of the respiratory chain in addition to F_oF_1-ATP synthase. The cells were fed by succinate and the ATP production by OXPHOS pathway was triggered. As the electrons flow through complexes II to IV, protons are simultaneously pumped into the matrix. This proton gradient was utilized by F_oF_1-ATP synthase to synthesize ATP from ADP and Pi (Besteiro *et al*., 2005).. Importantly, JK-11 inhibited this action by 86% at the concentration of 100 µM.

In conclusion, JK-11 doesn´t inhibit F_1-ATPase activity, but most likely inhibits the forward and reverse mode of the coupled F_oF_1 enzyme. Noteworthy, the used JK-11 concentration needed for inhibition of $\Delta\psi m$, ATP production and ATP hydrolysis was at least two times higher than measured EC_{50} values. Therefore, the inhibition of F_oF_1-ATP synthase/ATPase might not be the main mode of action in trypanosome cells. Most likely, JK-11 targets other cellular processes (e.g., the deoxyhypusine hydroxylase) and F_oF_1-ATPase is not the primary target of this compound in BF *T. brucei* cells.

6. References

1 Abbruzzese, A.; Park, M. H.; Folk, J. E. Deoxyhypusine hydroxylace from rat testis. Partial purification and characterization. J. Biol. Chem. 1988, 261, 3085–3089.

2 Abrahams JP, Leslie AG, Lutter R, Walker JE. Structure at 2.8 Å resolution of F1-ATPase from bovine heart mitochondria. Nature 1994, 370: 621-628.

3 Acestor N, Zíková A, Dalley RA, Anupama A, Panigrahi AK, Stuart KD. Trypanosoma brucei Mitochondrial Respiratome: Composition and Organization in Procyclic Form. Molecular & Cellular Proteomics: MCP. 2011;10(9):M110.006908. doi:10.1074/mcp.M110.006908.

4 Alsford S, Horn D. Single-locus targeting constructs for reliable regulated RNAi and transgene expression in Trypanosoma brucei. Mol Biochem Parasitol. September 2008;161(1): doi:10.1016/j.molbiopara.2008.05.006.

5 Bason JV (2008) Studies of the regulation and the catalytic mechanism of ATP synthase. Cambrigde, Disertation (Ph.D.). University of Cambridge. Faculty of biology.

6 Bacchi CJ, Nathan HC, Hutner SH, McCann PP, Sjoerdsma A. Polyamine metabolism: a potential therapeutic target in trypanosomes. Science. 1980 Oct 17;210(4467):332-4.

7 Balabaskaran NP, Dudkina NV, Kane LA, van Eyk JE, Boekema EJ,Mather MW. Highly Divergent Mitochondrial ATP Synthase Complexes in Tetrahymena thermophila. PLoS Biol 2010, 8(7): e1000418. doi:10.1371/journal.pbio.1000418

8 Balabaskaran NP, Morrisey JM, Ganesan SM, Ke H, Pershing AM, Mather MW, Vaidya AB. ATP Synthase Complex of Plasmodium falciparum: DIMERIC ASSEMBLY IN MITOCHONDRIAL MEMBRANES AND RESISTANCE TO GENETIC DISRUPTION. The Journal of Biological Chemistry 2011, 286(48), 41312–41322. doi:10.1074/jbc.M111.290973.

9 Besteiro S, Barrett MP, Riviere L, Bringaud F. Energy generation in insect stages of Trypanosoma brucei: metabolism in flux. Trends Parasitol 2005, 21: 185–191. pmid:15780841 doi: 10.1016/j.pt.2005.02.008.

10 Bowler MW, Montgomery MG, Leslie AG, Walker JE. How azide inhibits ATP hydrolysis by the F-ATPases. PNAS USA 2006, 103: 8646–8649. pmid:16728506 doi: 10.1073/pnas.0602915103.

11 Boyer PD. The ATP synthese – a splendid molecular machine. Annu. Rev. Biochem. 1997, 66:717–49

12 Brown SV, Hosking P, Li J, Williams N. ATP synthase is responsible for maintaining mitochondrial membrane potential in bloodstream form Trypanosoma brucei. Eukaryot Cell 2006, 5: 45–53. pmid:16400167 doi: 10.1128/ec.5.1.45-53.2006.

13 Bringaud F, Peris M, Zen KH, Larry Simpson L. Characterization of two nuclear-encoded protein components of mitochondrial ribonucleoprotein complexes from Leishmania tarentolae, Molecular and Biochemical Parasitology, Volume 71, Issue 1, April 1995, Pages 65-79, ISSN 0166-6851, http://dx.doi.org/10.1016/0166-6851(95)00023-T.

14 Brun R, Hecker H, Lun ZR. Trypanosoma evansi and T. equiperdum: distribution, biology, treatment and phylogenetic relationship (a review). Vet Parasitol 1998, 79: 95–107. pmid:9806490 doi: 10.1016/s0304-4017(98)00146-0

15 Capaldi RA, Schulenberg B, Murray J, Aggeler R. Cross-linking and electron microscopy studies of the structure and functioning of the Escherichia coli ATP synthase. J Exp Biol. 2000 Jan; 203(Pt 1):29-33.

16 Cardol P, González-Halphen D, Reyes-Prieto A, Baurain D, Matagne RF, Remacle C. The Mitochondrial Oxidative Phosphorylation Proteome of*Chlamydomonas reinhardtii* Deduced from the Genome Sequencing Project.*Plant Physiology*. 2005;137(2):447-459. doi:10.1104/pp.104.054148.

17 Coustou V, Biran M, Breton M, Guegan F, Riviere L, Plazolles N, Nolan D, Barrett MP, Franconi JM, Bringaud F. Glucose-induced remodeling of intermediary and energy metabolism in procyclic Trypanosoma brucei. J Biol Chem. 2008;283:16342–16354.

18 Coustou V, Besteiro S, Biran M, Diolez P, Bouchaud V, Voisin P, Michels PAM, Canioni P, Baltz T, Bringaud. ATP Generation in the Trypanosoma brucei Procyclic Form. J Biol Chem.2003, 278: 49625-49635.

19 Collinson IR, Runswick MJ, Buchanan SK, Fearnley IM, Skehel JM, van Raaij MJ, Griffiths DE, Walker JE. Fo membrane domain of ATP synthase from bovine heart mitochondria: purification, subunit composition, and reconstitution with F1-ATPase. Biochemistry 1994. 33: 7971-7978.

20 Chaudhuri M, Ajayi W, Hill GC. Biochemical and molecular properties of the Trypanosoma brucei alternative oxidase. Mol Biochem Parasitol. 1998, 95: 53-68.

21 Chen Y, Hung CH, Burderer T, Lee GS. Development of RNA interference revertants in Trypanosoma brucei cell lines generated with a double stranded RNA expression construct driven by two opposing promoters. Mol Biochem Parasitol 2003, 126: 275–279. pmid:12615326 doi: 10.1016/s0166-6851(02)00276-1.

22 Classen JB; Mergner WJ; Costa M. ATP hydrolysis by ischemic mitochondria. JOURNAL OF CELLULAR PHYSIOLOGY 1989, 141, 1, 53-59.

23 Dean S, Gould MK, Dewar CE, Schnaufer AC. Single point mutations in ATP synthase compensate for mitochondrial genome loss in trypanosomes. PNAS USA 2013;110(36):14741-14746. doi:10.1073/pnas.1305404110.

24 De Greef C, Hamers R, The serum resistance-associated (SRA) gene of Trypanosoma brucei rhodesiense encodes a variant surface glycoprotein-like protein, Molecular and Biochemical Parasitology, Volume 68, Issue 2, December 1994, Pages 277-284, ISSN 0166-6851, http://dx.doi.org/10.1016/0166-6851(94)90172-4.

25 Devenish RJ, Prescott M, Rodgers AJW. The Structure and Function of Mitochondrial F1F0-ATP Synthases. Int Rev Cell Mol Biol. 2008, 267: 1-58.

26 Dickson VK, Silvester JA, Fearnley IM, Leslie AG, Walker JE. On the structure of the stator of the mitochondrial ATP synthase. EMBO J. 2006, 25: 2911

27 Durand-Dubief M, Kohl L, Bastin P. Efficiency and specificity of RNA interference generated by intra- and intermolecular double stranded RNA in Trypanosoma brucei. Mol Biochem Parasitol. 2003;129:11–21.

28 Fairlamb AH, Henderson GB, Cerami A. Trypanothione is the primary target for arsenical drugs against African trypanosomes. PNAS USA 1989;86(8):2607-2611.

29 Fang J, Beattie DS. Identification of a gene encoding a 54 kDa alternative NADH dehydrogenase in Trypanosoma brucei. Mol. Biochem. Parasitol. 2003, 127, 73–77. http://dx.doi.org/10.1016/S0166-6851(02)00305-5.

30 Goebel T, Ulmer D, Projahn H, Kloeckner J, Heller E, Glaser M, Ponte-Sucre A, Specht S, Sarite SR, Achim Hoerauf A, Kaiser A, Hauber I, Hauber J, Holzgrabe U. Journal of Medicinal Chemistry 2008, 51 (2), 238-250 DOI: 10.1021/jm070763y.

31 Hannaert V, Bringaud F, Opperdoes FR, Michels PA. Evolution of energy metabolism and its compartmentation in Kinetoplastida. Kinetoplastid Biol Dis 2003, 2: 11. pmid:14613499 doi: 10.1186/1475-9292-2-11.

32 Hashimi H, Benkovicova V, Cermakova P, Lai DH, Horvath A, *et al*. The assembly of F_1F_o-ATP synthase is disrupted upon interference of RNA editing in Trypanosoma brucei. Int J Parasitol 2010, 40: 45–54. doi: 10.1016/j.ijpara.2009.07.005. pmid:19654010.

33 Horn D, McCulloch R. Molecular mechanisms underlying the control of antigenic variation in African trypanosomes. Current Opinion in Microbiology. 2010;13(6):700-705. doi:10.1016/j.mib.2010.08.009.

34 Jamonneau V, Ilboudo H, Kabore J, Kaba D, Koffi M, Solano P, Garcia A, Courtin D, Laveissière C, Lingue K, Büscher P, Bucheton B. Untreated human infections by Trypanosoma brucei gambiense are not 100% fatal. PLoS Negl Trop Dis 2012, 6: e1691. doi: 10.1371/journal.pntd.0001691. pmid:22720107

35 Kennedy PGE. Clinical features, diagnosis, and treatment of human African trypanosomiasis (sleeping sickness), Lancet Neurol 2013; 12: 186–94. doi:10.1016/S1474-4422(12)70296-X.

36 Kieft R, Capewell P, Turner CMR, Veitch NJ, MacLeod A, Hajduk S. Mechanism of Trypanosoma brucei gambiense (group 1) resistance to human trypanosome lytic factor. PNAS USA. 2010;107(37):16137-16141. doi:10.1073/pnas.1007074107.

37 Kovarova J, Horakova E, Changmai P, Vancova M, Lukes J. Mitochondrial and nucleolar localization of cysteine desulfurase Nfs and the scaffold protein Isu in Trypanosoma brucei. Eukaryot Cell 2014, 13: 353–362. doi: 10.1128/EC.00235-13. pmid:24243795.

38 LaCount DJ, Bruse S, Hill KL, Donelson JE, Double-stranded RNA interference in Trypanosoma brucei using head-to-head promoters, Molecular and Biochemical Parasitology, Volume 111, Issue 1, November 2000, Pages 67-76, ISSN 0166-6851, http://dx.doi.org/10.1016/S0166-6851(00)00300-5.

39 Lardy H, Reed P, Lin CH. Antibiotic inhibitors of mitochondrial ATP synthesis. Fed Proc. 1975 Jul;34(8):1707-10.

40 Law RH, Manon S, Devenish RJ, Nagley P. ATP synthase from Saccharomyces cerevisiae. Methods Enzymol 1995, 260: 133–163.

41 Lukeš J, Hashimi H, Verner Z, Číčová Z. The remarkable mitochondrion of trypanosomes and related flagellates. In: W. de Souza (Ed.), Structures and Organelles in Pathogenic Protists. Microbiology Monographs 2010, 17. Springer-Verlag, Berlin,: 227–252.

42 Mazet M, Morand P, Biran M, Bouyssou G, Courtois P, *et al*. Revisiting the central metabolism of the bloodstream forms of Trypanosoma brucei: production of acetate in the mitochondrion is essential for parasite viability. PLoS Negl Trop Dis 2013, 7: e2587. doi: 10.1371/journal.pntd.0002587. pmid:24367711.

43 Michels PA, Michels JP, Boonstra J, Konings WN (1979) Generation of an electrochemical proton gradient in bacteria by the excretion of metabolic end products. FEMS Microbiology letters, 5(5), 357-364.

44 Mitchell P, Chemiosmotic coupling in oxidative and photosynthetic phosphorylation, Biochimica et Biophysica Acta (BBA) - Bioenergetics, Volume 1807, Issue 12, December 2011, Pages 1507-1538, ISSN 0005-2728, http://dx.doi.org/10.1016/j.bbabio.2011.09.018.

45 Nelson RE, Aphasizheva I, Falick AM, Nebohacova M, Simpson L. The I-complex in Leishmania tarentolae is an uniquely-structured F1-ATPase. Molecular & Biochemical Parasitology 2004. 135, 219–222 Short communication

46 Njiokou F, Laveissère C, Simo G, Nkinin S, Grèbaut P, Cuny G, Herder S: Wild fauna as a probable animal reservoir for Trypanosoma brucei gambiense in Cameroon. Infect Gen Evol 2006, 6:147–153.

47 Njiokou F, Nimpaye H, Simo G, Njitchouang GR, Asonganyi T, Cuny G, Herder S: Domestic animals as potential reservoir hosts of Trypanosoma brucei gambiense in sleeping sickness foci in Cameroon. Parasite 2010, 17:61–66. 23.

48 Nolan DP, Voorheis HP. The mitochondrion in bloodstream forms of Trypanosoma brucei is energized by the electrogenic pumping of protons catalysed by the F1F0-ATPase. Eur. J. Biochem. 1992, 209 : 207-216.

49 Opperdoes FR, Borst P, Bakker S, Leene W. Localization of glycerol-3-phosphate oxidase in the mitochondrion and particulate NAD+-linked glycerol-3-phosphate dehydrogenase in the microbodies of the bloodstream form of Trypanosoma brucei. Eur. J. Biochem 1977. 76:29–39).

50 Park MH, Wolff EC. Separation of protein substrate and enzyme and identification of 1,3-diaminopropane as a product of spermidine cleavage. J. Biol. Chem. 1988, 263, 15264–15269.

51 Perez E, Lapaille M, Degand H, Cilibrasi L, Villavicencio-Queijeiro A, Morsomme P, Gonzalez-Halphen D, Field MC, Remacle C, Baurain D, Cardol P. The mitochondrial respiratory chain of the secondary green alga Euglena gracilis shares many additional subunits with parasitic Trypanosomatidae Mitochondrion 2014, Volume 19, Part B, November 2014, Pages 338-349, ISSN 1567-7249, http://dx.doi.org/10.1016/j.mito.2014.02.001.

52 Pholig G, Bernhard S, Blum J, Burri C, Mpanya Kabeya A, Fina Lubaki JP, Mpoo Mpoto A, Fungula Mununguu B, Kambau Manesa Deo G, Nsele Mutantu P, Mbo Kuikumbi F, Fukinsia Mintwo A, Kayeye Mununguu A, Dala A, Macharia S, Miaka Mia Bilenge C, Kande Betu Ku Mesu V, Ramon Franco J, Dieyi Dituvanga N, OlsonC. Phase 3 trial of pafuramidine maleate (DB289), a novel, oral drug, for treatment of first stage sleeping sickness: safety and efficacy, abstr. 542. 57th Meet. Am. Soc. Trop. Med. Hyg. 2008, New Orleans.

53 Räz B, Iten M, Grether-Bühler Y, Kaminsky R, Brun R. The Alamar Blue® assay to determine drug sensitivity of African trypanosomes (T.b. rhodesiense and T.b. gambiense) in vitro, Acta Tropica, Volume 68, Issue 2, November 1997, Pages 139-147, ISSN 0001-706X, http://dx.doi.org/10.1016/S0001-706X(97)00079-X.

54 Rubinstein JL, Walker JE, Henderson R. Structure of the mitochondrial ATP synthase by electron cryomicroscopy. EMBO J. 2006, 22: 6182-6192.

55 Schnaufer A, Clark-Walker GD, Steinberg AG, Stuart K. The F1-ATP synthase complex in bloodstream stage trypanosomes has an unusual and essential function. EMBO J 2005, 24: 4029–4040. pmid:16270030 doi: 10.1038/sj.emboj.7600862.

56 Schnaufer A, Domingo GJ, Stuart K. Natural and induced dyskinetoplastic trypanosomatids: how to live without mitochondrial DNA, International Journal for Parasitology, Volume 32, Issue 9, August 2002, Pages 1071-1084, ISSN 0020-7519, http://dx.doi.org/10.1016/S0020-7519(02)00020-6.

57 Simarro PP, Diarra A, Ruiz Postigo JA, Franco JR, Jannin JG. The Human African Trypanosomiasis Control and Surveillance Programme of the World Health Organization 2000–2009: The Way Forward. PLoS Negl Trop Dis 2008, 5(2): e1007. doi:10.1371/journal.pntd.0001007.

58 Simpson AG, Roger AJ. Protein phylogenies robustly resolve the deep-level relationships within Euglenozoa. Mol Phylogenet Evol 2004, 30: 201—212.

59 Simpson L, Sbicego S, AphasizhevR. Uridine insertion/deletion RNA editing in trypanosome mitochondria: A complex business. RNA 2003, 9(3), 265–276. doi:10.1261/rna.2178403.

60 Simpson L, Thiemann OH, Savill NJ, Alfonzo JD, Maslov DA. Evolution of RNA Editing in Trypanosome Mitochondria". Proc. Natl. Acad. Sci. USA 2000. 97, 6986-6993.

61 Speijer D; Breek CKD, Muijsers AO *et al*. Characterization of the respiratory chain from cultured Crithidia fasciculata. Molecular and biochemical parasitology 1997. 85 (2), 171-186.

62 Stuart KD. Evidence for the retention of kinetoplast DNA in an acriflavine-induced dyskinetoplastic strain of Trypanosoma brucei which replicates the altered central element of the kinetoplast. J Cell Biol 1971, 49: 189–195. pmid:4102002 doi: 10.1083/jcb.49.1.189.

63 Stuart K, Brun R, Croft S, Fairlamb A, Gürtler RE, McKerrow J, Reed S, Tarleton R. Kinetoplastids: related protozoan pathogens, different diseases. The Journal of Clinical Investigation 2008, 118 (4), 1301–1310. doi:10.1172/JCI33945.

64 Šubrtová K, Pannicusi B, Zíková A. ATPaseTb2, a Unique Membrane-bound FoF1-ATPase Component, Is Essential in Bloodstream and Dyskinetoplastic Trypanosomes. PLoS Pathog 2015, 11(2):e1004660. doi: 10.1371/journal.ppat.1004660.

65 Thomson R, Samanovic M, Raper J. Activity of trypanosome lytic factor: a novel component of innate immunity. Future microbiology. 2009;4:789-796. doi:10.2217/FMB.09.57.

66 van Lis R, Mendoza-Hernandez G, Groth G, Atteia A. New insights into the unique structure of the F_oF_1-ATP synthase from the chlamydomonad algae Polytomella sp. and Chlamydomonas reinhardtii. Plant Physiol 2007, 144: 1190–1199. pmid:17468226 doi: 10.1104/pp.106.094060.

67 Vázquez-Acevedo M, Cardol P, Cano-Estrada A, Lapaille M, Remacle C, González-Halphen D. The mitochondrial ATP synthase of chlorophycean algae contains eight subunits of unknown origin involved in the formation of an atypical stator-stalk and in the dimerization of the complex. Journal of Bioenergetics and Biomembranes 2006, 38, Issue 5-6, 271-282.

68 Velours J, Arselin G. The Saccharomyces cerevisiae ATP synthase. J Bioenerg Biomembr. 2000;32:383–390.

69 Verner Z, Čermáková P, Škodová I, Kriegová E, Horváth A, Lukeš J. Complex I (NADH:ubiquinone oxidoreductase) is active in but non-essential for procyclic Trypanosoma brucei, Molecular and Biochemical Parasitology, Volume 175, Issue 2, February 2011, Pages 196-200, ISSN 0166-6851, http://dx.doi.org/10.1016/j.molbiopara.2010.11.003.

70 von Ballmoos C, Cook GM, Dimroth P. Unique rotary ATP synthase and its biological diversity. Annu Rev Biophys 2008. 37: 43–64.: DOI: 10.1146/annurev.biophys.37.032807.130018.

71 Walker JE, Collinson IR. The role of the stalk in the coupling mechanism of F1F0-ATPases. FEBS Letters 1994, 346: 39-43.

72 Walker JE, Dickson VK. The peripheral stalk of the mitochondrial ATP synthase. Biochim Biophys Acta 2006, 1757: 286–296. pmid:16697972 doi: 10.1016/j.bbabio.2006.01.001.

73 Walker JE, Saraste M, Gay NJ. The unc operon. Nucleotide sequence, regulation and structure of ATP-synthase. Biochim Biophys Acta. 1984a Sep 6;768(2):164-200. Review.

74 Zíková A, Schnaufer A, Dalley RA, Panigrahi AK, Stuart KD. The F_oF_1-ATP synthase complex contains novel subunits and is essential for procyclic Trypanosoma brucei. PLoS Pathog 2009, 5: e1000436. doi: 10.1371/journal.ppat.1000436. pmid:19436713.